# Functional analysis of cardiomyocytes carrying mutations in *SCN5A* gene

Master's thesis
Anna-Maria Linnoinen
Faculty of Medicine and Biosciences
University of Tampere
January 2017

# Pro gradu – tutkielma

Paikka: TAMPEREEN YLIOPISTO
Lääketieteen ja biotieteiden tiedekunta
Tekijä: LINNOINEN, ANNA-MARIA ELISABET
Otsikko: *SCN5A* mutaatiota kantavien sydänsolujen solujen toiminnalliset analyysit
Sivumäärä: 64
Ohjaajat: Katriina Aalto-Setälä, Eeva Laurila
Tarkastajat: Professori, MD Katriina Aalto-Setälä, Apulaisprofessori Heli Skottman
Päiväys: 26.01.2017

---

**Tutkimuksen tausta ja tavoitteet:** Sydämen toiminta perustuu elektrokemiallisiin muutoksiin sydänlihassolujen kalvojen lävitse. Näitä elektrokemiallisia virtoja kutsutaan aktiopotentiaaleiksi. Ne johtavat kalsiumin vapautumiseen solunsisäisistä varastoista, kalsiumin sitoutumiseen sarkomeerisiin proteiineihin ja lopulta sydänlihaksen supistumiseen. Natrium, kalsium ja kalium ovat tärkeimmät ionit, aktiopotentiaalin kannalta. Nopeat natriumvirrat sydänlihassoluissa saavat aikaan solukalvon depolarisaation.

*SCN5A* on geeni, joka sijaitsee kromosomissa 3p21. Se koodittaa sydänlihassoluissa ekspressoituvaa jänniteherkkää $Na_v1.5$-natriumkanavaa, josta natrium virtaa sydänlihassolun sytoplasmaan. Potilaat, joilla on *SCN5A* mutaatio, ilmenee erilaisia vakavia sydämen rytmihäiriösairauksia, kuten pitkä QT-oireyhtymä (LQT) ja Brugada syndrooma (BrS).

Tämä tutkimus keskittyy kahteen eri *SCN5A* mutaatioon: I141V ja R1913C. Tutkimuksen tavoitteena oli: 1) Lepotilanteessa *SCN5A* mutaatiosolujen sykkeen karakterisointi. 2) Tutkia *SCN5A*-mutaatiosolujen lääkevastetta 3) Kuvata ja analysoida visuaalisesti ja Beatview-ohjelman avulla *SCN5A*-mutaatiosolut ja kontrollisolut 4) Saada tietoa SCN5A-mutaatiosoluista, joita ei ole mahdollista analysoida Beatview-ohjelman avulla.

**Menetelmät:** Kaksi solulinjaa erilaistettiin potilaista, joilla *SCN5A*-geenin mutaatio ja niitä verrattiin terveisiin kontrollisoluihin. Jokaisen linjan solujen käyttäytymistä analysoitiin kuvaamalla yksittäisiä, erilaistettuja, sykkiviä sydänlihassoluja. *SCN5A*-geenin mutaatiota kantavilla potilailla esiintyy rytmihäiriöitä rasituksen yhteydessä. Adrenaliinia käytettiin ilmentämään tätä *in vitro*-soluviljelyolosuhteissa. Flekainidin vaikutusta tutkittiin sydänsolujen rytmihäiriöihin. Sydänsolujen luokittelu ja analysointi suoritettiin visuallisesti ja käyttämällä Beatview-ohjelmaa.

**Tutkimustulokset:** *SCN5A*-mutaatiosolujen syketaajuus oli korkeampi kuin kontrollisoluilla. Flekainidi laski syketaajuutta jokaisen solulinjan soluilla ja teki tautisoluista tasaisemmin sykkiviä. Adrenaliini ei nostanut sykettä oletuksen mukaisesti johtuen todennäköisesti korkeasta leposykkeestä. Beatview-ohjelman ja visuaalisen analysoinnin tulokset olivat samankaltaisia.

**Johtopäätökset:** Kuten voitiin olettaa, *SCN5A* solujen sykkiminen oli epäsäännöllisempää kuin kontrollisolujen ja lisäksi niiden syketiheys oli korkeampi. Tautisolujen relaksaatio-aika oli myös kontrollisoluja lyhyempi. Flekainidi hidasti *SCN5A* solujen syketiheyttä ja nosti relaksaatioaikaa kaikilla solulinjoilla.

# Master's thesis

Place: UNIVERSITY OF TAMPERE
Faculty of Medicine and Biosciences
Author: LINNOINEN, ANNA-MARIA ELISABET
Title: Functional analysis of cardiomyocytes carrying mutations in *SCN5A* gene
Pages: 64
Supervisors: Katriina Aalto-Setälä, Eeva Laurila
Reviewers: Professor, MD Katriina Aalto-Setälä, Associate Professor Heli Skottman
Date: 26.01.2017

---

**Background and aims:** Heart function is based on electrochemical changes (action potentials) across the cardiomyocyte cell membranes. Action potentials induces the release of calcium ions from intracellular stores (sarcoplasmic reticulum), binding of calcium to sarcomeric proteins and finally in cardiac muscle contraction. The most important ions, which take part in the action potential generation, are sodium, calcium and potassium. The rapid flow of sodium ions into the cardiomyocytes causes the depolarization of the cell membrane.

*SCN5A* is the gene located on chromosome 3p21, and it encodes the pore-forming α-subunit of the voltage-gated sodium channel $Na_v1.5$. Patients with these mutations in SCN5A gene have different inherited arrhythmia syndromes, such as congenital long QT syndrome (LQTS) and Brugada syndrome (BrS).

This work will focus on two different *SCN5A* mutations, I141V and R1913C. It has different aims: 1) Baseline beating characterization of cardiomyocytes carrying mutation in *SCN5A*. 2) To study drug responses of cardiomyocytes carrying mutation in *SCN5A*. 3) Image and analyse both visually and using the BeatView software SCN5A mutation –patient specific and wildtype (WT) iPSC –derived cardiomyocytes (CMs) 4) To get reliable data of SCN5A mutation –patient specific CMs visual inspection was used, if it is impossible to analyze signals with BeatView.

**Methods:** Two of cell lines were derived from patients with mutations in the *SCN5A* gene and they were compared to a control cell line from a healthy individual. Behavior of the cells were analyzed using videos of single dissociated beating cardiomyocytes of each cell line. Individuals carrying mutations in the *SCN5A* gene get arrhythmias during exercise. Adrenaline was used to replicate this phenomenon *in vitro*. Flecainide was used to study how it effects in good way to arrhythmic symptoms of the CMs. Analyzing and classification of CMs were studied both visually and using Beatview software.

**Results:** Beating frequency of cells with SCN5A mutations was higher than in control cells. Flecainide decreased beating frequency of all cell lines and made disease cells more regular. Adrenaline did not increase beating frequency in SCN5A cells as assumed most likely due to high baseline beating frequency. Similar beating behavior were obtained whether the analysis was done by visual analyzing or by using Beatview software.

**Conclusions:** *SCN5A* cells beating behaviors were more arrhythmic than control cells and beating frequencies was also higher than in control cells. Time cells were relaxed was shorter time than in control cells. Flecainide slowed down the beating frequency and increased time cells were relaxed in all cell lines.

# Acknowledgements

This study was carried out in Heart Group, University of Tampere, BioMediTech. First of all, I would like to thank the leader of the Heart group, Katriina Aalto-Setälä, and my instructor, Eeva Laurila. You consistently allowed this paper to be my own work, but steered me in the right the direction whenever you thought I needed it. Also, I would like to thank other members of the Heart group for advice and support, especially Henna Lippi, Markus Haponen, Risto-Pekka Pölönen and Chandra Prajapati. You all were always near whenever I ran into a trouble spot or has a question about my research or writing. Without your passionate participation and input, the validation survey could not have been successfully conducted.

Finally, I must express my very profound gratitude to my family and all of my friends for providing me with unfailing support and continuous encouragement throughout my years of study and through the process of researching and writing this thesis. This accomplishment would not have been possible without you all. Thank you.

Tampere 26.01.2017

Anna-Maria Linnoinen

# Sisällysluettelo

# Abbreviations

| | |
|---|---|
| AP | Action potential, AP |
| ADRA1 | Adrenoceptor Alpha 1, ADRA1 |
| ADRA1A | Adrenoceptor Alpha 1A |
| ATP | Adenosine triphosphate |
| AV | Atrioventricular |
| AVN | Atrioventricular node |
| bFGF | Basic fibroblast growth factor |
| BMP | Bone morphogenetic protein |
| BPM | Beats per minute |
| BrS | Brugada syndrome |
| CDC | Conduction defect disease |
| CICR | Calcium-induced calcium-release |
| CM | Cardiomyocyte |
| cMyBP-C | Cardiac myosin binding protein C |
| c-Myc | Myelocytomatosis viral oncogene homolog |
| CPVT | Catecholaminergic polymorphic ventricular tachycardia |
| cTnC | Cardiac troponin C |
| DMEM | Dulbecco's Modified Eagle-medium |
| EB | Embryoid body |
| ECG | Electrocardiography |
| END-2 | Mouse visceral endodermal-like |
| FGF | Fibroblast growth factor |
| hESC | Human embryonic stem cell |
| hiPSC | Human induced pluripotent stem cell |
| $I_{Ca}$ | Calcium channel |
| $I_{Ca}$, L | Long-lasting (L)-type calcium channel |
| $I_{Ca}$, T | Low-voltage-activated (T)-type calcium channel |
| iCM | Induced cardiomyocyte-like cell |
| iPS cell | Induced pluripotent stem cell |
| I141V | Isoleucine to Valine substitution at position 141 |
| Klf4 | Kruppel-like factor 4 |
| JNK | C-Jun N-terminal kinase |
| KO | Knockout, |
| KO-SR | Knockout serum replacement-medium |
| LQTS | Long QT syndrome |
| LQT3 | Long QT syndrome type 3 |
| MEF | Mouse embryonic fibroblast |
| MHC | Myosin heavy chains |
| MLC2 | Artrial myosin light chain |
| miRNA | Micro RNA |
| mRNA | Messenger RNA |
| ms | Milliseconds |

| | |
|---|---|
| $Na_v$ | Voltage-gated sodium channels |
| NEAA | Nonessential amino acids |
| NCX | $Na^+/Ca^{2+}$-exchanger |
| Nkx2.5 | NK2 transcription factor related gene, locus 5 |
| Oct4 | Octamer-binding transcription factor 4 |
| qPCR | Quantitative polymerase chain reaction |
| QTc | Corrected QT-interval |
| P | Pacemaker |
| PCR | Polymerase chain reaction |
| PKA | Protein kinase A |
| PKC | Protein kinase C |
| ROCK | Rho-associated protein kinase |
| ROI | Region of interest |
| RyR | Ryanodine receptor |
| R1913C | Arginine to cysteine changing at R1913C position |
| *SCN5A* | Sodium voltage-gated channel alpha subunit 5 |
| SERCA | Sarco/endoplasmic reticulum Ca2+-ATPase |
| SN | Sinoatrial node |
| Sox2 | Sex determining region Y-box 2 |
| SR | Sarcoplasmic reticulum |
| SRF | Serum response factor |
| Tbx5 | T-box transcription factor 5 |
| TdP | Torsades de Pointes |
| TM | Transmembrane |
| VSD | Voltage-sensing domain |
| WNT | Wingless/INT protein |
| WT | Wild type |

# 1. Introduction

Since 1995, many mutations in the genes coding for cardiac ion channel subunits or proteins interacting with ion channels, were described in patients with a number of inherited arrhythmia syndromes (Swan et al. 2014). *SCN5A* encodes for the α-subunit of the cardiac voltage-gated sodium channel Nav1.5 (Butters et al. 2010). The voltage-gated sodium channels ($Na_{v)}$ in CM play key roles in cells' accomplishments to generate and transmit electrical signals like action potential (AP). Dysfunction of these channels is typically caused by mutations in the *SCN5A* gene. (Remme, 2013.)

Patients with mutations in *SCN5A* gene have different inherited arrhythmia syndromes, such as congenital long QT syndrome (LQTS) and Brugada syndrome (BrS) (Remme, 2013). In the end of 2014, Swan and colleagues reported the new point mutation of *SCN5A* gene. They noticed that this new mutation is connected to the ventricular tachycardia during exercise. (Swan et al. 2014.)

Takahashi and Yamanaka published a new way to create pluripotent stem cells by inducing mouse embryonic or adult fibroblasts using retroviral vector carrying transcription factors in 2006 (Takahashi & Yamanaka, 2006). After this remarkable finding, the same has been obtained with human somatic cells by several research groups all over the world (Kujala et al. 2012; Lan et al. 2013; Sun et al. 2012). Including CMs, human induced pluripotent stem cells
(hiPSCs) can be differentiated into any cell type of the human body (Mummery et al. 2012). hiPSCs can be used as a useful platform for cardiac disease modeling and -drug screening, because there are no many human sources of cardiac tissue samples available. However, hiPSC derived CMs are structurally and functionally immature. (Keung et al. 2014; Robertson et al. 2013.)

In this study, baseline beating characterization and drug responses on *SCN5A* mutation – patient specific and wild type (WT) hiPSC –derived CMs were studied. Three cell lines were used. Two of these cell lines are derived from patients with mutations I141V or R1913C in the *SCN5A* gene and they will be compared to a control cell line from a healthy individual. Behavior of the cells were analyzed using videos of beating cardiomyocytes of each cell line.

Beatview software was used to analyzing and visual analysing was used to get reliable data of CMs, which are impossible to analyze with BeatView.

# 2. Literature review

## 2.1 Introduction to cardiac muscle and cardiomyocytes

### 2.1.1 The structure of heart and cardiac cells

The cardiac muscle, *myocardium* can be divided into four chambers: left atrium, left ventricle, right atrium and right ventricle (Figure 1) (Bjålie et al. 2008; Heikkilä et al. 2008). It has four valves: two of atrioventricular (AV) valves, which are between the upper chambers (atria) and lower chambers (ventricles) and two valves between chambers and arteries (Figure 1) (Bers 2001; Severs, 2000). Heart's role is to pump oxidized blood to peripheral circulation and deoxidized blood to the pulmonary circulation. Valves allow blood to flow in only one direction through the heart. The tissue surrounding the cardiac muscle cells is rich in collagen fibrils and other components of connective tissue and blood vessels and nerves. (Bjålie et al. 2008; Heikkilä et al. 2008.)

In addition to the *myocardium*, the heart contains also two others tissues, which form the heart wall together with *myocardium* (Bjålie et al. 2008; Heikkilä et al. 2008). The inner layer is the *endocardium*, which is covered by endothelial cells. The outer layer of the heart wall, *epicardium* is surrounded by mesothelial cells. *Myocardium's* structure is elongated and its contraction capable cells are linked to each other. It is composed of CMs, fibroblasts and smooth muscle cells. (Heikkilä et al. 2008.) There are different types of CMs in the myocardium: atrial and ventricular CMs, pacemaker cells, in the sinoatrial node (SN) and Purkinje fiber cells (Bootman et al. 2006; Dehaan & Eichna, 1961; Moorman & Christoffels, 2003; Severs, 2000). Different CMs contribute to structural, biochemical, mechanical and electrical properties of the functional heart. Atrial and ventricular CMs form the muscular walls of the heart. Pacemaker cells and Purkinje fibers in the conduction system are specialized cardiomyocytes that generate and conduct electrical impulses. The SN is composed of a group of pacemaker cells, resides in the right atrium generating impulses to initiate heart contraction. The atrioventricular node (AVN) is located between the atria and ventricles, and it conducts an electrical impulse from the atria to the ventricles. (Bjålie et al. 2008; Heikkilä et al. 2008.)

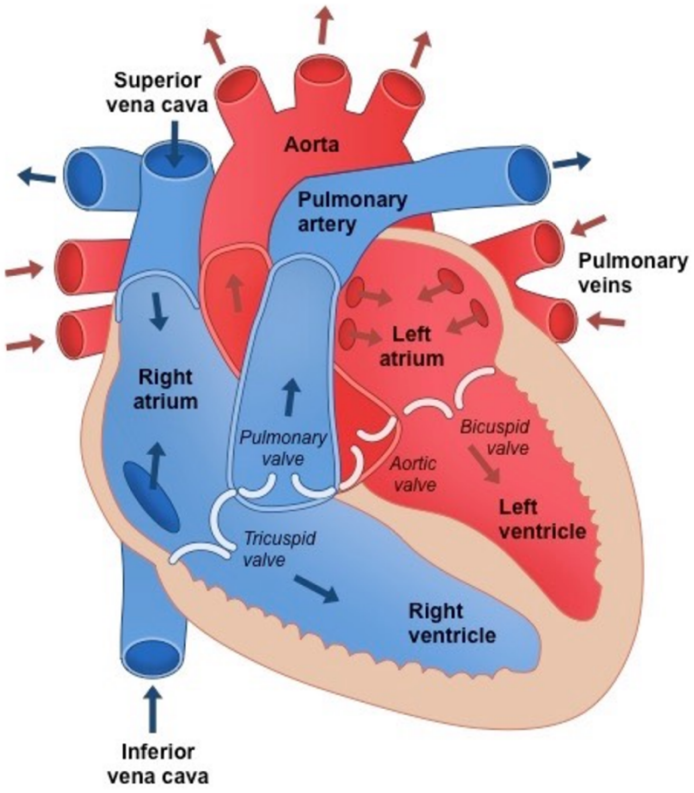


**Figure 1.** The heart can be divided into four chambers: left atrium, left ventricle, right atrium and right ventricle. It has four valves, two atrioventricular (AV) valves: mitral valve and tricuspid valve and two valves between chambers and arteries: aortic valve and pulmonary valve (Texas Heart institute).

A typical single ventricular cell is 50-150 μm long and 10-20 μm wide but atrial cells are slightly smaller. More than half of the content of the cells is contracting protein material. It is organized as hundreds separated filaments, myofibrils, which extend from one end of the cell to the other. (Bjålie et al. 2008; Heikkilä et al. 2008.)

Every myofibril consists of molecular structures, *sarcomeres* that are responsible for the contraction of the cell. Sarcomeres are formed by thick and thin myofilaments and Z-discs (Figure 2). They are tightly organized to allow strong cell contraction. The length of the sarcomere increases from stretched state to extreme contraction from 2.2 μm to 1.6 μm. (Bjålie et al. 2008; Heikkilä et al. 2008.)

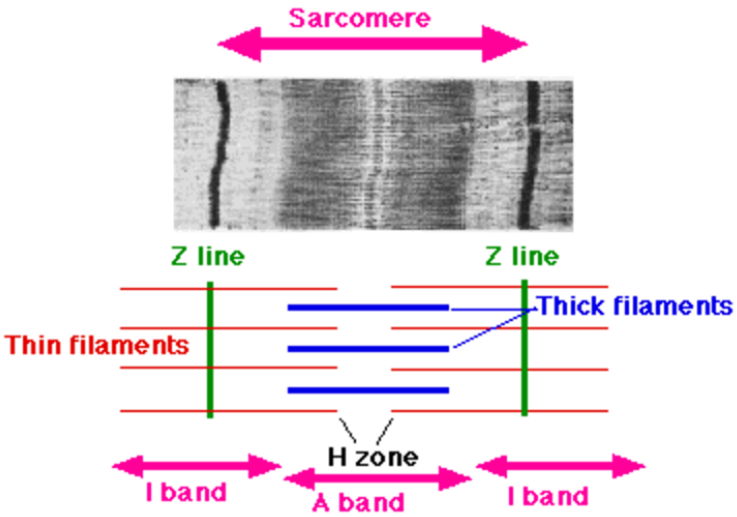


**Figure 2.** Sarcomere structure. Sarcomeres are formed by thick and thin myofilaments and Z-discs. Surrounding the Z-line is the region of the I-band and One A-band contains the entire length of a single thick filament. (Microscopic Muscle Structure.)

Myosin and actin are the most important sarcomeric proteins of which the filaments are formed (Chiu et al. 2010; Clark et al. 2002; Heikkilä et al. 2008). Furthermore, titin (also known as connectin) is also important connecting protein in sarcomeres. Every thick myofilament consists of hundreds of myosin molecules. (Harris et al. 2011; Heikkilä et al. 2008.) They are connected to each other by cardiac myosin binding protein C (cMyBP-C). A myosin molecule consists of two myosin heavy chains (MHC) and two pairs of different type of myosin light chains (MLC1 and MLC2). Actin molecules form thin myofilaments together with protein parts including group of troponin and tropomyosin molecules. (Bers, 2001; Heikkilä et al. 2008; Tardiff, 2011).) Actin molecule has a special structure for myosin head in order to bind myosin and thus to allow the contraction of the sarcomere (Barefield et al. 2014; Heikkilä et al. 2008).

### 2.1.2 Electrophysiology of cardiomyocytes, cardiac action potential

The function of the heart is based on electrochemical changes across the cardiomyocyte membranes. Cardiomyocytes have a remarkable property called electrical excitability. In this, depolarization of the membrane above a threshold voltage triggers a spontaneous all-or-none response called action potential. This electric activity of the heart can be measured from the entire human heart by recording ECG. (Boron & Boulpaep, 2009; Heikkilä et al. 2008.)

Electrocardiography (ECG) is one of the most important and most widespread methods to explore the electrical activity of the heart using electrodes placed on the patient's body (Boron & Boulpaep, 2009; Heikkilä et al. 2008). In ECG, first wave describes activations of the atria and it is named as P wave (Figure 3). The first part of P wave describes the previously activated atria and latter part the left atria. Duration of the P wave indicates and represents the time that it takes to atrial depolarization. (Kujala et al. 2012; Heikkilä et al. 2008.)

Activation of pacemaker cells in sinoatrial node (SN), does not show in the ECG, because of its resulting electrical current is so small. After this, the cardiac conduction system is activated: AV node, His bundle, conduction system and Purkinje fibers. Their activation no either shown in ECG. The next wave visible in the ECG is the QRS-complex (Figure 3), which arises of ventricular depolarization. This depolarization spreads rapidly through the cardiac muscle from epicardium to endocardium, and finally ventricular repolarization spreads slowly which can be seen as T wave in ECG (Figure 3). The source of the U wave is unknown. (Kujala et al. 2012; Bjålie et al. 2008; Heikkilä et al. 2008.)

In ECG, all of the P-waves and PQ-time (counted from the beginning of the P wave, Q wave to start) should be look similar. Shape, length, and direction of QRS-complex is analyzed. Its direction can be either positive or negative, depends on the angle of the heart is looked. The duration of the QRS-complex is normally less than 120 milliseconds and it is usually evaluated based on the width of the QRS-complex. Narrow complex can be a sign of atrial arrhythmias, while wide complex may mean ventricular arrhythmias. T-wave should be one top and in the same direction with QRS-complex. If there is variation of T-wave's form, it may refer to tendency of arrhythmia. Sometimes U-wave follow T wave but it is smaller and same direction with T wave. ST-segment is flat and at the same level with the base line. If the ST segment increases, it is often a warning sign of an impending myocardial damage and its decrease may be due to chronic ischemia. QT interval announces a slowdown or the acceleration of the rhythm depending on whether the time is short or prolonged. (Thaler, 1999.)

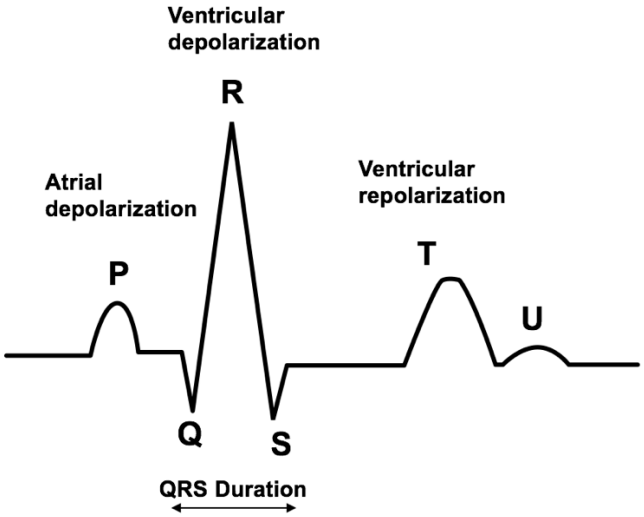


**Figure 3.** Schematic representation of ECG. ECG begins with the P wave caused by atrial depolarization. It is followed by the QRS complex, which is caused by ventricular depolarization and finally T wave, which represents the ventricular repolarization. The source of the U wave is unknown. (Heikkilä et al. 2008.)

Action potential is a transient, regenerative electrical impulse in which the membrane potential increases rapidly to a peak that is more positive than the normal, negative resting voltage (Bjålie et al. 2008; Heikkilä et al. 2008). The most important ions, which take the part in the action potential, are sodium, calcium and potassium. All these ions have their corresponding ion channels in the cell membrane. (Bjålie et al. 2008; Boron & Boulpaep, 2009; Heikkilä et al. 2008.) Electronic impulse is created at the top of the right sinoatrial node (SN). In SN, there is cardiac pacemaker (P) cells and they have spontaneous action potentials, which based on leaking calcium channels and cause diastolic depolarizations (Bjålie et al. 2008; Heikkilä et al. 2008). There are no fast sodium channels in the P cells and SN membrane voltage change toward to positive happens via calcium channels. Because of the pacemaker role of the SN, cardiomyocytes do not need external stimulation to trigger action potentials as neurons do. (Boron & Boulpaep, 2009; Bjålie et al. 2008; Heikkilä et al. 2008.)

The impulse generated in the same way repeatedly and causes the rhythmically repeated electromechanical activation of the heart, which is called the heart rate. Electric activation is mediated by specialized conduction system of the heart. The signal goes from the atria to the chambers and starts the cardiac muscle contraction. (Bjålie et al. 2008; Heikkilä et al, 2008.) Effective action requires mechanical ventricular activation after a suitable delay after activation of atria. For this reason, the electric excitation is markedly slower in the

atrioventricular node (AV node) than elsewhere in cardiac conduction system. Variability of the heart rate and cardiac contraction help the blood flow to adapt to the physiological requirements, such as maintaining homeostasis by equalizing the chemical characteristics (e.g. pH, and the number of ions) and to transport carbon dioxide to the lungs removing it from the body. (Kujala et al. 2012; Bjålie et al. 2008; Heikkilä et al. 2008.)

In axons, $Na^+$ channels are the most important ion channels in initiating action potentials and generating fast propagating spikes. However, $Ca^{2+}$ channels often cause a more sustained depolarizing current, which is the reason for the long-life action potentials observed in cardiac cells. The action potential causes releasing of calcium ions from intracellular stores (sarcoplasmic reticulum) and thus the cardiac muscle contraction. Figure 4 presents how cardiac AP can be divided into five phases. (Boron & Boulpaep, 2009; Heikkilä et al. 2008.)

The cell membrane is electrically polarized so that there are negative charges inside the cell in relation to the outside of the cell. Between these two sides, a so-called membrane voltage potential is normally an average of -90 mV (Figure 4). (Bjålie et al. 2008; Heikkilä et al. 2008.) When the membrane voltage decreases below -60 mV, the cell membrane will be quickly completely depolarized (Phase 0) (Figure 4). After this threshold is exceeded, cell membrane passes more $Na^+$ ions and the membrane potential becomes less negative due to this ion flow. When it reaches the level of -75 mV, all of the voltage-gated $Na^+$ channels open and $Na^+$ ions flow into the cell very quickly. Increased membrane voltage level of 30 mV leads to closing of the $Na^+$ channels. The higher the diastolic membrane potential, the faster is the Phase 0 of the action potential. (Heikkilä et al. 2008.)

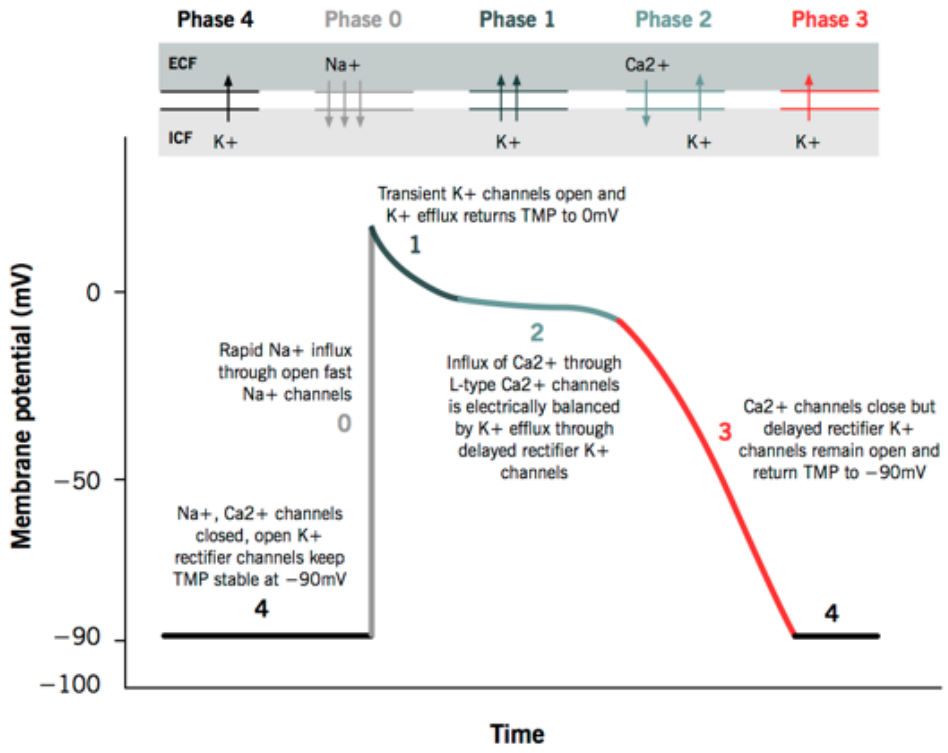


**Figure 4.** Cardiac action potential can be divided into five phases: 0) stimulation and rising phase, 1) increasing repolarization phase, 2) plateau phase, 3) repolarizing phase and 4) resting potential. (McMaster Pathophysiology Review: picture bank).

Local voltage changes in the cell membrane cause opening of the adjacent sodium channels. They continue to spread the voltage change along the cell membrane. In the ventricle muscle, action potential spreads via gap junctions from one cardiomyocyte to another, eventually reaching the last cell. (Boron & Boulpaep, 2009.)

Repolarization (Phase 0) starts when depolarization has reached its peak and $Na^+$ flows stops. Repolarization means the recovery of the cell membrane to negative resting potential. When $Na^+$ channels are closed, $K^+$ ions stabilize plateau phase (Phase 2) and start to flow outside of the cell and extracellular $Cl^-$ ions to inside the cell. (Boron & Boulpaep, 2009.) This causes opening of voltage-dependent calcium channel ($I_{Ca}$) and $Ca^{2+}$ ions start to flow into the cardiomyocytes from extracellular space (Figure 5). There are two different type of $I_{Ca}$: Long-lasting (L)-type ($I_{Ca}$, L) and low-voltage-activated (T)-type ($I_{Ca}$, T). (Bers 2000; Bers 2001; Bers, 2008.)

When $I_{Ca}$ receptors have been activated, intracellular $Ca^{2+}$ levels increase and it leads to activation of ryanodine receptors (RyRs) (Figure 5). This causes $Ca^{2+}$ flux out of the inner

storage, the sarcoplasmic reticulum (SR) and the process is called calcium-induced calcium-release (CICR) (Figure 5) (Bers, 2002.). Increasing of cytoplasmic $Ca^{2+}$ concentration make $Ca^{2+}$ ions available to bind to troponin C molecules in the actin filaments. This interaction allows actin and myosin binding together and thereby the contraction of the whole sarcomere. Calcium enters mitochondria via uniporter and is removed by NCX (Figure 5). (Heikkilä et al. 2008.)

When the $Ca^{2+}$ ions are released from the troponin C molecules, the cardiomyocyte relaxes. This occurs when the cytoplasmic $Ca^{2+}$ concentration is decreased by the sarcoplasmic reticulum $Ca^{2+}$ ATPase (SERCA). This pumps $Ca^{2+}$ ions back to SR and $Na^{+}/Ca^{2+}$ exchanger pushes them out of the cell. This cytoplasmic $Ca^{2+}$ concentration lowering causes the cardiomyocyte relaxation. (Bers 2000; Bers 2001; Bers, 2008.)

When membrane voltage reaches -50 mV level, outflow of the $K^{+}$ ions increases, repolarization speeds up (Phase 3) (Figure 4) and membrane potential returns to -90 mV resting level. Finally, ion concentrations of the resting phase return with the sodium-potassium exchange pump system and calcium pump system using ATP as the energy source. (Bjålie et al. 2008; Heikkilä et al, 2008.)

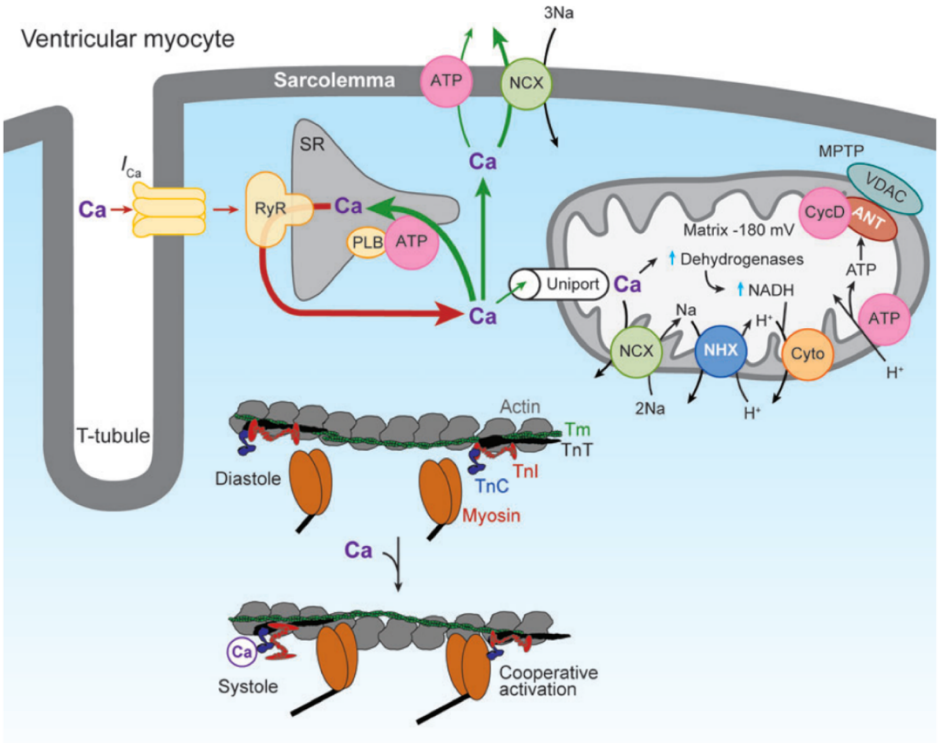


**Figure 5.** Schematic presentation of calcium transport. Calcium flow into cell via $I_{ca}$ activates sarcoplasmic reticulum (SR) and release via the ryanodine receptor (RyR) which leads to activation of contraction. SR Ca-ATPase uptakes SR calcium and extrusion via Na/Ca exchange (NCX) permits relaxation. Phospholamban (PLB) regulates the activity of SR Ca-ATPase. In cytoplasm, free calcium binds to troponin C (TN) on the thin filaments and permits the myofibrillar contraction. Calcium enters mitochondria via uniporter and is removed by NCX. Calcium in mitochondria activates ATP production. Na-K ATPase and Na/H exchanger contribute to the ion balance and potential of the cell. Protons (H+) are pumped out of mitochondria by the cytochrome (Cyto). (Bers, 2008.)

## 2.2 *SCN5A* gene and $Na_v$ channels

*SCN5A* encodes for the α-subunit of the cardiac voltage-gated sodium channel Nav1.5 (Butters et al. 2010). These channels control the flow of $Na^+$ ions into cells that initiates the depolarizing Phase 0 of the cardiac action potential (Liu et al. 2014). The voltage-gated sodium channels ($Na_v$) in CM play key roles in cells' accomplishments to generate and transmit electrical signals like AP (Remme, 2013).

The biophysical properties of the $Na_v$ are complex (Liu et al. 2014). Dysfunction of these channels is typically caused by mutations in the *SCN5A* gene. It is located in the chromosome 3p21 and encodes the major cardiac sodium channel $Na_v1.5$. (Remme, 2013.) The $Na_v1.5$ channel α subunit forms the ion-conducting pore and changes structural conformation of the

channel according to membrane potential. This process is called voltage-depend gating. (Liu et al. 2014.)

$Na_v$ channels are monomers with four repetitive transmembrane domains (DI-DIV), containing six transmembrane (TM) segments (S1-S6) (Amarouch et al. 2014; Chen-Izu et al. 2015). The first four TM segments (S1-S4) include the voltage-sensing domain (VSD) and last two TM segments (S5 and S6) form the pore of the channel when assembled in a tetrameric configuration. The α subunit has an intracellular N-terminus and C-terminus and four homologous domains (I-IV). (Boron & Boulpaep, 2009.) Furthermore, α subunit interacts also with four single β subunits (β1-4) and they play a role in modulating channel gating or channel expression. The α and β subunits form a macromolecular complex with other proteins and that modulates channel expression and function (Figure 6). (Liu et al. 2014.)

Since 1995, many mutations in the genes coding for cardiac ion channel subunits or proteins interacting with ion channels, were described in patients with a number of inherited arrhythmia syndromes (Swan et al. 2014). These syndromes include congenital long QT syndrome (LQTS), Brugada syndrome (BrS), and catecholaminergic polymorphic ventricular tachycardia (CPVT) and progressive cardiac conduction defect disease (CCD), (Swan et al. 2014; Obeyesekere et al. 2015). There have been also cases describing not the only one of these diseases, but combined phenotypes such BrS+CCD or BrS+LQTS (Obeyesekere et al. 2015).

In the end of 2014, Swan and colleagues reported a novel point mutation of *SCN5A* gene. They noticed that this new mutation is connected to the ventricular tachycardia during exercise. (Swan et al. 2014.) Also in many other inherited forms of arrhythmic disorders, such as LQT, BrS and CPVT, similar symptoms have been reported (Wilde & Brugada, 2011). This kind of symptoms are life-threatening because ventricular tachycardia causes decreasing of blood pressure, losing consciousness and can lead to death without resuscitation (Swan et al 2014).

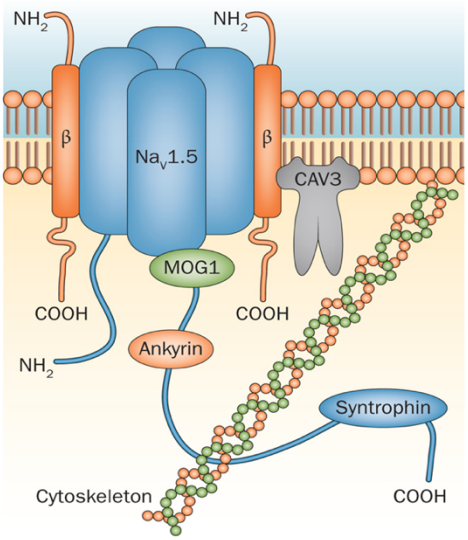


**Figure 6**. Structure of $Na_v1.5$ channel complex, which is part of a macromolecular complex. The α subunit, which is $Na_v1.5$ channel, interacts with multiple cellular proteins, including accessory proteins such as β subunits, ankyrin, CAV3, MOG1, syntrophin, and cytoskeleton at the cell membrane. (Liu et al.2014.)

## 2.3. Genetic cardiac diseases due mutations in *SCN5A* gene

### 2.3.1. LQTS

As mentioned before, the QT interval describes the time to beginning of ventricular depolarization to the end of its repolarization (Heikkilä et al. 2008). Long-QT syndrome (LQTS) is a cardiovascular disorder characterized by an abnormality in cardiac repolarization leading to a prolonged QT interval and T wave on the patient's ECG (Figure 7) (Splawski et al. 2000; Hedley et al. 2009). The patients with LQTS are predisposed to get ventricular tachyarrhythmias called Torsades de Pointes (TdP) (Kiviaho et al. 2015) and patients with these symptoms have increased risk for sudden death (Remme, 2013).

Various subtypes of LQTS are diagnosed with gene mutations in particular genes and there are enormous range of mutations in each gene (Kiviaho et al. 2015). Roughly 5–10 % of LQTS patients are carriers of a gain-of-function mutation in *SCN5A*, the gene encoding the a-subunit of the LQT3 subtype (Malan et al. 2015). Patients with LQTS type 3 (LQT3, associated with *SCN5A* mutations) present arrhythmias predominantly during rest or sleep at slow heart rates, and they are often relatively bradycardic LQT3 patients are especially at risk

for sudden death compared to other subtypes, and the first clinical symptom diagnosed is often cardiac arrest.

LQT3 patients typically have defects in fast inactivation of the sodium current, allowing for sodium channels to re-open, resulting in a continuous (late) inside flow during the AP plateau phase. (Remme, 2013.)

In diagnostics, prolongation of the QT interval is estimated corrected for heart rate. It is calculated using Bazett's equation. In the ECG, QTc values over 450 ms in males and 460 ms in females can be considered as positive for LQTS. When the QT interval is longer than 500 ms, the risk for arrhythmias increases. (Vijayakumar et al. 2014.)

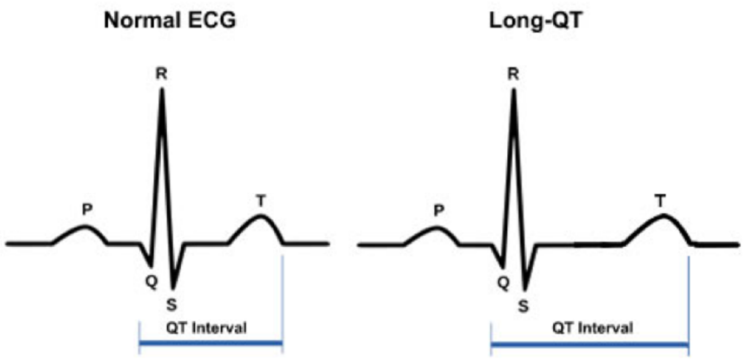


**Figure 7.** Comparison of a normal ECG compared to one with a prolonged QT interval. In ECG the interval from the begin of the Q wave to the end of the T wave is lengthened.

### 2.3.2. Brugada syndrome

In the last decade, studies have started to reveal the genetic background of diseases, which are characterized by serious ventricular arrhythmias and sudden death. Ten years ago, a new syndrome causing sudden cardiac deaths was discovered. (Brugada P & Brugada J, 1992, Heikkilä et al. 2008.) The syndrome was characterized in the ECG with a narrow right bundle branch block and a bulge of ST-segment in the right-hand side chest connections ($V_1$-$V_3$) (Figure 8) (Brugada et al, 2014). The syndrome was named Brugada syndrome, according to its discoverer Pedro Brugada (Escárcega et al, 2009). Congenital defect of the ion channel was also the cause of Brugada syndrome, where the *SCN5A* mutations have been shown to cause the syndrome. Consequences of the mutation can be seen as disrupted sodium ion

channel activity and weakened flow of the sodium ions. The effect is strongest' in the right ventricle, which explains the ECG finding especially in the right sided chest connections. Weakened flow of the sodium shortens the action potential and causes potential differences during systole in different areas of the heart, and thus exposes to cardiac arrhythmias either during sleep or rest. This can lead to sudden death at worst. (Heikkilä et al. 2008.)

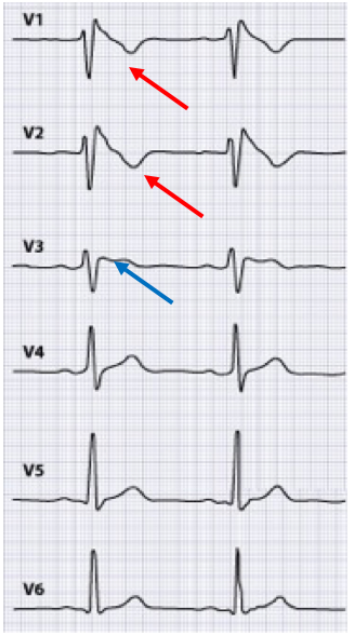


**Figure 8.** Typical ST-segment in $V_1$-$V_3$ coupling in Brugada syndrome. This presents typical findings of patient's ECG with Brugada syndrome. Red narrows in $V_1$ and $V_2$ coupling show negative T-wave and blue narrow presents a gradually descending ST-segment. (Heikkilä et al. 2008.)

### 2.3.3. CPVT type of phenotype

CPVT is characterized by episodic syncope occurring during exercise or acute emotion in individuals without structural cardiac abnormalities. These attacks cause ventricular fibrillation and can lead to momentary loss of consciousness or cause sudden death. The mean age of onset of symptoms (usually a syncopal episode) is at school age. The heart is structurally sound and in diagnostic imaging there is anything unusual and resting ECG is normal. If CPVT in untreated, it is highly lethal and sudden death May be the first manifestation of the disease. (Swan et al.1999.)

## 2.4. *SCN5A* mutations

*SCN5A* gene mutations have been associated with long QT syndrome (LQTS) type 3, Brugada syndrome (BrS), sick sinus syndrome, and cardiac conduction disease (CCD) (Bennett et al. 1995; Chen et al. 1998; Jiang et al. 1994). *SCN5A*-E1784K is the most common mutation associated with BrS and LQTS3 (Veltmann et al. 2016). Table 1 presents some of the common *SCN5A* mutations and cardiac phenotypes of them.

**Table 1.** *SCN5A* mutations and their phenotypes

| ***SCN5A* mutation** | **Cardiac phenotype** |
|---|---|
| S216L, K480N, A572D, F816Y, G983D, **P141V** | LQT |
| S216L, S262G, K480N, A572D, F816Y, G983D, and T1526P | Remain as variants of unknown significance |
| R568H and A993T | Pathogenic LQTS3 causing mutations |
| R222stop, R2012H, **R1913C** | BrS |

The R1913C mutation has unknown pathological significance, but it is known that amino acid arginine (R) changes to cysteine (C) at position 1913. A heart disorder characterized by LQT interval on the ECG and polymorphic ventricular arrhytmias. Mutation has been localized on C-terminus. (Uniprot.) Figure 8 shows localization of this mutation in the $Na_v1.5$ channel.

In the I141V mutation, amino acid isoleucine (I) is substituted to valine (V) at position 141 (Amarouch et al, 2014). Figure 9 presents localization of this mutation in $Na_v1.5$ channel. This mutation of $Na_v$ causes several clinical hyper-excitability phenotypes. Channel window current increases due to mutation, while action potential simulations suggested that it lowered the excitability threshold of cardiac cells. This predisposes to ventricular extrasystole and ventricular fibrillation. (Swan et al. 2014.)

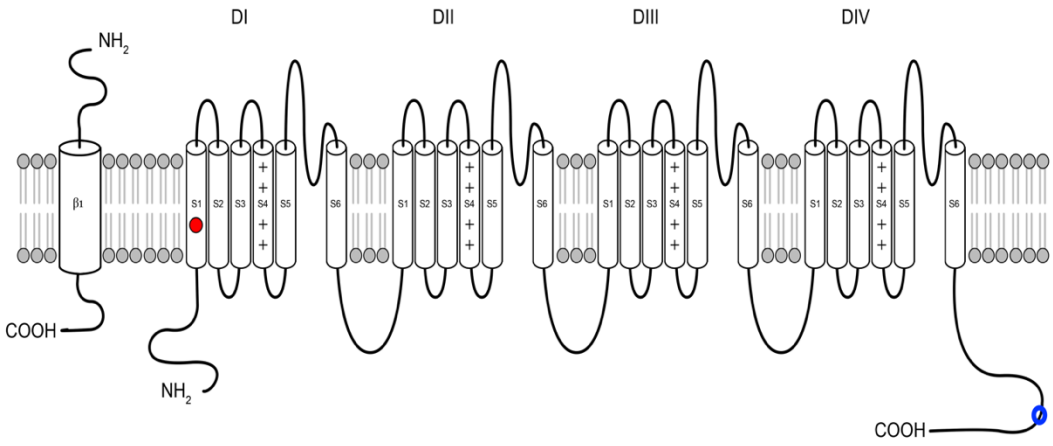


**Figure 9.** Opened structure of $Na_v1.5$ channel in the cell membrane (Figure modified from Remme, 2013). Location of p.I141V mutation is marked with red circle and p.R1913C mutation with blue circle. $Na_v$ channel has four identical parts (DI-DIV) and all of these consist of six transmembrane segments (S1-S6). There are also four single β subunits, β1-4, of which the first one is shown in the Figure. (Boron & Boulpaep, 2009.)

## 2.5. Induced pluripotent stem cells

In the 2007, Shinya Yamanaka showed with his research group that it is possible to reprogram a human somatic cell to a pluripotent stem cell. This can be achieved using a retroviral vector carrying four transcription factors, which are required for induction of pluripotency: Oct-3/4, Sox2, c-Myc and KLF4. These cells, acting like artificial human embryonic stem cells (hES) were named induced pluripotent stem cells (iPS cells). Human iPS cells (hiPCs) are able to divide indefinitely and to form all cell types of the body, like embryonic stem cells. (Takahashi et al. 2007.)

hiPSCs have similar morphology, proliferation, surface antigens, gene expression, epigenetic status of pluripotent cell-specific genes, and telomerase activity like ESs have. hiPS cells can be prepared also for example from dermal fibroblasts of adult human who has mutation and with this method produced cells can be differentiated into the desired functional cells (Figure 10). Also, they allow development of patient or disease specific cell lines. This offers a great tool to study the disease phenotypes, because the original mutation genotype remains in the cells *in vitro.* (Takahashi et al. 2007.)

hiPSCs are very useful to study genetically inherited diseases affecting tissues which are difficult to access, such as the heart. Myocardial biopsy has a high risk for the patient. Many

cardiovascular and neural diseases have been studied using hiPSCs. These include for example Long-QT –syndromes, catecholaminergic polymorphic ventricular tachycardia, Alzheimer's, Huntington's diseases and Parkinson's disease. Furthermore, in addition to the Yamanaka's original method using integrating retroviral vectors, reprogramming can also be achieved by using non-integrative vectors, synthetic mRNAs and small molecules. With these novel techniques, it is possible to avoid insertional mutagenesis and transgene reactivation and thus minimize the risk of tumor formation, cancer risk and variability between generated cell lines. (Bellin et al. 2012.)

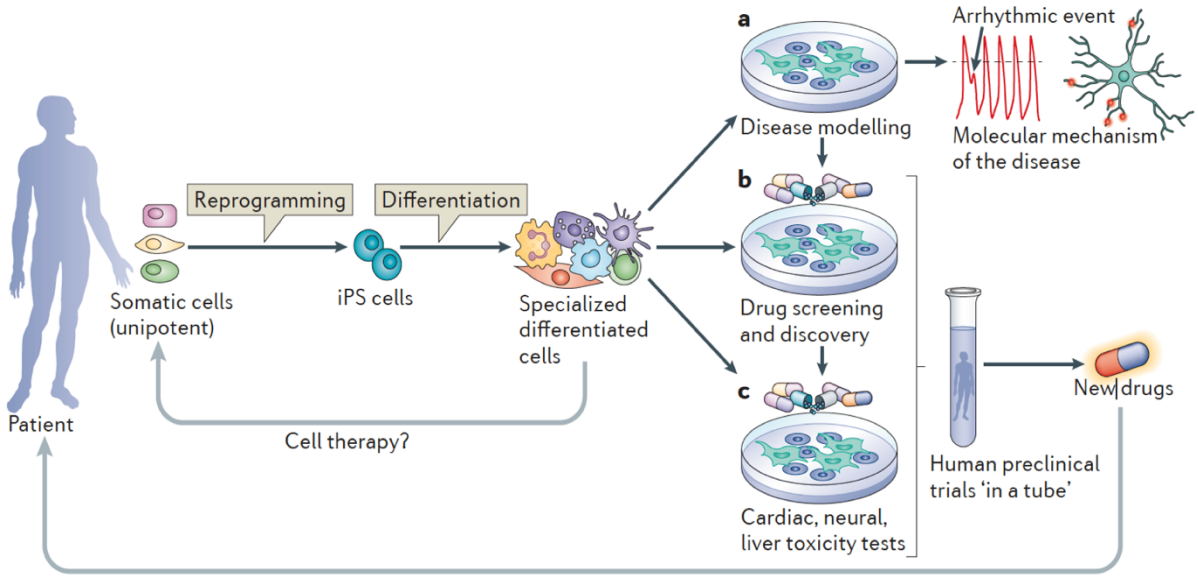


**Figure 10.** Schematic picture presents how adult somatic cells can be reprogrammed into human induced pluripotent stem cells (hiPSC) (Bellin et al. 2012). After *in vitro* differentiation, human iPS cells (hiPSCs) can be used for many different applications. **a)** hiPSCs can be used to study disease phenotypes to understand for example the molecular causes for arrhythmias in cardiomyocytes or for defects in neurogenic differentiation. **b)** drug screening and discovery is another application for hiPS cells. With hiPSCs, it is possible to discover novel candidate drugs and compounds and to identify target pathways. **c)** hiPS cells have important role in cardiac, neural and liver toxicity tests. With these tests, are possible to estimate cellular toxic responses. Drug screening and toxicity tests typify human preclinical "trials in a tube" together and that enable the introduction of "the patient" in early stages of the drug discovery process. (Bellin et al. 2012.)

## 2.6. hiPSC derived cardiomyocytes

The successful differentiation of human embryonic stem cells (hESCs), and more recently, of hiPSCs, into functional cardiomyocytes, has opened new opportunities for cardiovascular research and therapies (Mummery et al. 2012). hiPSC differentiation is similar to the embryonic development (Bellin et al. 2012) and they can be differentiated into any somatic cell of the human body, including CM with different reprogramming methods (Mummery et al. 2012).

Cardiogenesis, the differentiation of CMs and mesoderm formation is controlled by three families of protein growth factors: Bone morphogenetic proteins (BMPs), the wingless/INT proteins (WNTs) and the fibroblast growth factors (FGFs). These growth factors and their inhibitors are expressed in endoderm and they started the cardiac transcriptional program, which leads to proliferation and maturation of CMs. (Mummery et al. 2012.)

Usually, BMP signaling promotes cardiogenesis, as well as FGFs. The function of WNT proteins is more complex and the effects to cardiogenesis dependent on the signaling pathway. WNT proteins acting via β-catenin/GSK3 inhibit cardiogenesis, while the acting via PKC/JNK (Protein kinase C/ c-Jun-N-terminal kinase) pathway promotes cardiogenesis. When the mesoderm cells have acquired the necessary signals, the necessary CMs differentiation genes are activated in their genome. Then the cells begin to differentiate and expresses typical transcription factors of the heart cells. For example, homeodomain transcription factor Nkx2-5, the T-box protein Tbx5 are early markers of the cardiac lineage that are activated during the formation of the heart fields. They work together with GATA transcription factors and serum response factor (SRF) to activate cardiac structural genes, such as myosin light and heavy chains, troponins and desmin. (Mummery et al. 2012.)

The possibilities to produce CMs *in vitro*, helps to study cardiac diseases. Cardiac research has been difficult with unsuitable animal models (mostly rodents with extremely high beat rates) and limited amounts of biopsies and tissue samples. Stem cell derived CMs offer an unlimited amount of research material. There are many different ways to differentiate CMs: embryoid body (EB) method; monolayer culture; inductive co-culture and a new feeder-free small molecule method. (Mummery et al. 2012; Lian et al. 2013.)

In the EB method, hiPSCs are either fully dissociated and cultured on special modelling plates or partly dissociated and cultured on standard cell culture plates to control EB formation. EBs are able to form all three germ layers (ectoderm, endoderm and mesoderm). They develop into spheroids, 3D-structures of aggregated pluripotent stem cells and they develop beating CMs spontaneously. hiPSCs are dissociated and plated as monolayers or matrix sandwich using Matrigel cell culture plates in monolayer culture method. With monolayer method, diffusion of nutrition and growth factors is more controlled and reproducible. (Mummery et al. 2012.)

Inductive co-culture method using a mouse visceral endodermal-like (END-2) cells was described by Mummery and colleagues in 2003. This method uses their cell-signaling properties advance cardiogenesis (Mummery et al. 2003). In this method, hiPSC lines are differentiated by culturing them on top of END-2 cells. With the END-2 method, it is possible to get spontaneously beating differentiated CMs using quite small amounts of cells. (Mummery et al. 2012.)

Small molecular differentiation method is free of growth factors, and it is suitable for all existing human pluripotent stem cell lines. In this method, stem cells are differentiated to CMs completely defined and known conditions by temporal modulation of regulators of canonical WNTs. It is, therefore, a feeder-free method. (Lian et al. 2013.) Using of culture media containing unspecified or undisclosed components has limited the development of applications for pluripotent cells (Kusuda-Furue et al. 2010). Feeder cells of animal origin and other components using in cell culturing contain animal proteins and other molecules, that can move to stem cells during culturing (Ojala et al. 2012). Lack of knowledge of their responses to specific cues that control self-renewal, differentiation, and lineage selection (Kusuda-Furue et al. 2010). Therefore, this method will enable efficient production of human cardiomyocytes for development and disease research, drug screening and testing, and advancing cardiac cellular therapies (Lian et al. 2013).

Successful reprogramming of fibroblasts into induced cardiomyocyte-like cells (iCMs) without going through an intermediate progenitor or stem cell stage in murine and human models has been recently reported. This direct cardiac reprogramming is a potential method for regenerative medicine in the future and for dissecting the regulatory control of cell fate determination. (Srivastava & Yu, 2015.)

Moreover, it offers a new way to understand the transcription factor function and to study the complex interplay among transcriptional regulators, miRNAs, and epigenetic regulators (Sadahiro et al. 2015). Unlike iPSCs, the iCMs quickly exited the cell cycle and did not form colonies and it that is why it is faster method (Srivastava & Yu, 2015).

## 2.7. Drugs affecting cardiomyocyte function

Adrenaline is a hormone, neurotransmitter and it is also used as a medicine. One physiological stimulus to adrenaline secretion is during exercise. The body's circulatory system adrenaline directly affects both the α- and β-receptors via the indirectly through homeostatic reflexes. Adrenaline affects to cardiac adrenergic receptors and it leads to: 1) heart rate increases (= positive chronotropic effect), due to sinus node cell depolarization acceleration 2) atrial and ventricular contractile force increases (= positive inotropic effect); characterized by the systole is reduced and the volume increases heart rate, myocardial oxygen consumption increases significantly and thus the efficiency of the heart (work compared to oxygen consumption) decreases 3) impulse conduction velocity of heart increases 4) spontaneous activity of pacemaker cells in the chambers increase and this may lead to ventricular arrhythmias, for example extrasystole, tachycardia, and even fibrillation. (Oulu & Tuomisto, 2007.)

Flecainide slows down the fast sodium channels at the level of the atria, chambers, and Purkinje fibers. It does not significantly affect the action potential duration. Flecainide slows down conduction in the atrioventricular node and in particular bundle of His and Purkinje fibers. Flecainide does not affect the action potential duration. It slows conduction in the atria and in the atrioventricular node. However, slowing of the atrioventricular conduction affected mainly the His-Purkinje track. It extends the high-speed cable lines refractory in the atrioventricular node. This explains the effectiveness of flecainide in the treatment of supraventricular tachycardia. (Oulu & Tuomisto, 2007.)

Flecainide is used in clinical. In supraventricular tachycardia the recommended starting dose is 100 mg per day. A dose increase should be considered only after 4-5 days of treatment. The optimal dose is 200 mg per day. The maximum dose is 300 mg per day. In ventricular

tachycardia The usual dose is 200 mg per day. A dose increase should be considered only after 4-5 days of treatment. (Orion Pharma.)

# 3. Aims

This research project had two aims: At first study baseline beating characterization of cardiomyocytes carrying mutation in *SCN5A* using various methods to understand what kind of phenotypes cells have. And then to study drug responses of cardiomyocytes carrying mutation in *SCN5A* with different methods.

# 4. Materials and methods

## 4.1. Materials

### 4.1.1 Patient-specific hiPSC lines and culturing

Three cell lines were used in this study. Two of these cell lines were generated of a patient with *SCN5A* gene mutations. *UTA.11705.SCN5A cell line* was generated of a patient with I141V mutation and *UTA.13902.SCN5A* cell line of a patient with R1913C mutation. These two cell lines were compared to third cell line *UTA.04602.WT,* generated from a healthy individual. All hiPSC cell lines had been produced earlier in our research group according to the Yamanaka method, using either dermal fibroblasts or blood cells as starting material. In this method, four transcription factors are transfected into the cells (Oct4, Sox2, c-myc and Klf4). (Takahashi et al. 2007.) The collection of biopsies for generating patient specific hiPSC-lines was approved by the ethical committee of Pirkanmaa Hospital District (Aalto-Setälä R08070) and written informed consent was obtained from all of the patients.

The clinical phenotype of the patients included the following symptoms:
- I141V had increasing amount of ventricular extra beats during exercise, but no sudden cardiac death or unexplained death at young age has been presented in the family.
- R1913C presented Brugada type of ECG finding and the patient had been resuscitated during a marathon run. Subsequently he received and intracardiac defibrillator.

Human iPSCs characterization included verification of mutations by qPCR, karyotype analysis, verification of gene expression by PCR and protein expression by immunochemistry. These had been previously performed in our research group. hiPSCs were cultured on mouse embryonic fibroblasts (MEFs, 26 000 cells/$cm^2$, Merck Millipore, MA, USA). MEF division was stopped by using mitomycin-C. Therefore, they act as feeder cells to promote growth of undifferentiated hiPSCs and to keep their pluripotent state in hES-medium (Table 2).

**Table 2.** Mediums

**hES medium** (20% KO-SR DMEM). Pen/Strep = 10 U/ml Penicillin + 10 U/ml Streptomycin.

| ***Components*** | ***Quantity*** |
|---|---|
| Knock-Out DMEM (Life Technologies) | ad 100% |
| Knock-Out Serum Replacement (KO-SR, Life Technologies) | 20% |
| Non-essential amino acids (NEAA, Fischer Scientific) | 1% |
| GlutaMax (Life Technologies) | 2 mM |
| Penicillin Streptomycin (Pen Strep) (Fischer Scientific) (50 U/ml) | 0.25 ml |
| 2-mercaptoethanol (Life Technologies) | 0.1 mM |
| Basic fibroblast growth factor (bFGF, R&D Systems) | 4 ng/ml |

**END-2 medium**

| ***Components*** | ***Quantity*** |
|---|---|
| DMEM-F12 (Life Technologies) | ad 100% |
| FBS (Immunodiagnostic) | 7.5% |
| NEAA (Fischer Scientific) | 1% |
| GlutaMax (Life Technologies) | 2 mM |
| Penicillin Streptomycin (Pen Strep) (Fischer Scientific) (50 U/ml) | 0.25 ml |

**0% KO-SR hES medium**

| ***Components*** | ***Quantity*** |
|---|---|
| KO-DMEM (Life Technologies) | ad 100% |
| NEAA (Fischer Scientific) | 1% |
| GlutaMax (Life Technologies) | 2mM |
| Penicillin Streptomycin (Pen Strep) (Fischer Scientific) (50 U/ml) | 0,25 ml |
| 2-mercaptoethanol (Life Technologies) | 0.1mM |
| Ascorbic acid (Sigma Aldrich), added just before use | 3mM |

**10% KO-SR hES –medium**

| ***Components*** | ***Quantity*** |
|---|---|
| KO-DMEM (Life Technologies) | ad 100% |
| KO-SR (Life Technologies) | 10% |
| NEAA (Fischer Scientific) | 1% |
| GlutaMax (Life Technologies) (2mM) | 2 mM |
| Penicillin Streptomycin (Pen Strep) (Fischer Scientific) (50 U/ml) | 0.25 ml |

| | |
|---|---|
| 2-mercaptoethanol (Life Technologies) | 0.1 mM |

**RPMI+B27-medium**

| ***Components*** | ***Quantity*** |
|---|---|
| RPMI (Fischer Scientific) | ad 100% |
| B27 (Fischer Scientific) | 2% |
| Penicillin Streptomycin (Pen Strep) (Fischer Scientific) (50 U/ml) | 0.25 ml |

**EB –medium (20% FBS KO-DMEM)**

| ***Components*** | ***Quantity*** |
|---|---|
| KO-DMEM (Life Technologies) | 77.5% |
| FBS (Immunodiagnostic) | 20% |
| NEAA (Fischer Scientific) | 1% |
| Glutamax (Life Technologies) | 2 mM |

## 4.2 Methods

### 4.2.1 Cardiomyocyte differentiation

CM differentiation was performed using either END-2 co-culture or small molecule differentiation method.

#### 4.2.1.1 END-2 co-culture

To induce differentiation of hiPSCs into CMs, they were co-cultured with murine visceral endoderm-like (END-2) cells (prof. Mummery, Humbrecht Institute, Utrecht, The Netherlands). END-2 –cells were Mitomycin-C (Sigma Aldrich, MO, USA) inactivated (5 µl/ml, 3 hours), trypsinized (Lonza, Switzerland) and plated on 12-well-plate (Nunc) 175 000 cells/well in END-2-medium (Table 2). After overnight incubation (at 37°C), END-2 cells were attached and then 0% KO-SR hES medium (Table 2) was changed to them an hour before plating the hiPSCs. MEF cells were removed and hiPSC colonies were detached by scraping. hiPSC colonies were moved on END-2 cells (~30 colonies/well) with minimal amount of culture medium. Then cells were co-cultured in 37°C. At days 5, 8, and 12, 0% KO-SR hES-medium was changed and at day 14, the medium was changed to 10% KO-SR hES –medium (Table 2) and fresh medium was changed for the cells three times a week.

#### 4.2.1.2 Small molecule differentiation

Another method, which was used, is the small molecule differentiation method. It is a feeder-free method and it is suitable for all human pluripotent stem cells. With this method, it is possible to get monolayer cell mat. In small molecule differentiation, RPMI/B27 culture medium is used (Table 2). B27 is serum-free nutritional supplement. Insulin has been found to inhibit CMs differentiation during the first five days, so, during the differentiation B27 medium is used without insulin and after differentiation, insulin containing maintenance medium is used. (Lian et al. 2013.)

Differentiation is started at day -4 by transferring iPS cells from 6-well-plate to 12-well plates (Nunc). Old medium was removed and Accutase enzyme was added (1ml/well, incubated 8min at 37°C). After this, mTeSR™1 medium (1 ml/well) was added and the cells were flushed off the plate bottom and re-plated on 12-well-plate at 500 000-1 000 000 cells/well in mTeSR™1 medium with ROCK inhibitor. Medium was changed at days -3, -2 and -1.

At day 0, insulin-free RPMI/B27 medium (Table 2) with CHIR99021 reagent (12 µM/12-well-plate) was added. CHIR99021 reagent removed exactly 24 hours after it had been added and RPMI/B27 insulin-free medium was added in place of it. At day 3 IWP4 reagent (5 µM/12-well-plate) was added with RPMI/B27 insulin-free medium. Medium was changed at days 5. At day 7 and after it, fresh RPMI/B27 insulin-free medium was changed every third day.

Cells were monitored with phase-contrast microscopy using a Nikon Eclipse TS100 microscope with C-4xB/22 ocular and 4x/0.40 Ph1ADL objective (Nikon, Japan, Tokyo). At day 15, hiPSC colonies formed spontaneously beating areas in END2 differentiation methods and when using small molecule differentiation strong enough beating areas can be found at day 12.

### 4.2.2 Dissociation of beating cardiomyocytes

Before the video analysis, cells were dissociated, separated mechanically both growth plate and from each other to allow the recording and analysis of the single cells. At day 16 or later, beating areas of cell colonies were cut and separated with scalpel. They were collected in culture medium (10% KO-SR hES medium, (Table 2) and dissociated (Mummery et al. 2003). Beating areas were washed with Low-Ca (buffer 1) (Table 3) at RT for 30 minutes. After that, they were treated with collagenase A (Roche Diagnostics, Switzerland) (buffer 2) at 37 ˚C for 45 minutes to one hour. Cells were incubated in KB medium (buffer 3) (Table 3) at RT for one hour (1M glucose was added to buffer 20 µl to 1ml). Aggregates were resuspended in EB medium (20% FBS in KO-DMEM) (Table 2) by pipetting up and down against the bottom of the dish until clumps broke up. This helps aggregates to break into single cell suspension. Single cell suspension was plated to onto the wells of a 4-plate (one beating area/well).

After dissociation, the cells were allowed to settle bottom of the culture plate and attached into it. After one day, cells were attached and they were allowed to recover 2-3 days before video recording so that they are of uniform quality and beating better. EB medium was changed one day before video recording to enhance the beating.

**Table 3.** Components of dissociation buffers. Volumes are for making 100 ml of each buffer

| **Dissociation buffers** | | | |
|---|---|---|---|
| ***Components*** | **Low-Ca (Buffer 1)** | **Enzyme (Buffer 2)** | **KB (Buffer 3)** |
| NaCl | 12ml (1M) | 12ml (1M) | - |
| $CaCl_2$ | - | 3 µl (1M) | - |
| $K_2HPO^4$ | - | - | 3 ml |
| KCL | 0.54 ml (1M) | 0.54 ml (1M) | 8.5 ml (1M) |
| $Na_2ATP$ | - | - | 2mmol/L |
| $MgSO_4$ | 0.5 ml (1M) | 0.5 ml (1M) | 0.5 ml (1M) |
| EGTA | - | - | 0.1 (1M) |
| Na Pyruvate | 0.5 ml (1M) | 0.5 ml (1M) | 0.5 ml (1M) |
| Glucose | 2 ml (1M) | 2 ml (1M) | 2 ml (1M) |
| Creatine | - | - | 5 ml (0.1M) |
| Taurine | 20ml (1M) | 20ml (1M) | 20ml (0.1M) |
| Collagenase A | - | 1 mg/ml | - |
| HEPES | 1ml (1M) | 1 ml (1M) | - |
| $H_2O$ | ad 100 ml | ad 100 ml | ad 100 ml |
| pH correction | NaOH | NaOH | - |
| pH | 6.9 | 6.9 | 7.2 |

4.2.3 Video recording of the CMs

On the day of use, coverslip (5 mm diameter), containing the dissociated hiPSC-derived CMs, was mounted to an RC-25 recording chamber (Warner Instruments Inc.) and an inverted Olympus IX71 microscope (Olympus Corporation) with using UApo/340 x20 air objective (Olympus Corporation). CMs were continuously perfused with perfusate medium (Table 4). pH of the perfusate medium was set to 7.4 with NaOH and preheated to 35-36◦ C by an SH-27B inline-heater controlled by a TC-324B unit (all from Warner Instruments Inc., Hamden, USA). The perfusion flow was controlled by a gravity driven VC3 8 application system (ALA Scientific Instruments Inc., NY, USA).

CMs in the coverslips were perfused before experimental recordings about 10-15 minutes so that the cells became accustomed to fluid flow, perfusate medium and changing conditions. A

high-speed camera (Imperx model GEV-B1620M-TC000, Imperx, United States, Florida) was connected to microscope to record spontaneously beating CMs for 30 seconds using 60 fps imaging parameters with JAI Control Tool software. Cells to be recorded were selected visually. Requirements for selecting a cell were that the beating is strong enough and steady, movement is clearly visible and estimated beating frequency is at least close to the physiological range.

**Table 4.** Perfusion liquid components of 500 ml liquid

| **Perfusion liquid** | |
|---|---|
| ***Components*** | **Quantity** |
| NaCl | 71.5 ml (1M) |
| KCL | 2.4 ml (1M) |
| $MgCl_2$ | 0.9 ml (1M) |
| Glucose | 0.6 ml (1M) |
| HEPES | 2.5ml (1M) |
| $H_2O$ (Millipore) | ad 500ml |

4.2.3.1 Drug experiments of *UTA.04602.WT* cell line

Selected beating areas were cut, dissociated and plated on coverslips. Dissociation was done 7 days before imaging experiments. EB-culture medium (Table 2) was changed just once in week, one day before imaging. This cell line's cells were used 25 and 32 days after differentiation to ensure that they are usable and strong enough for video recording.

Data of the control cell line was collected by taking baseline imaging with perfusate medium and after it with 10 µM concentrations of flecainide (Figure 10A). To get this concentration, 100 µl of 5 mM flecainide was dissolved to 50 ml of perfusate medium (Table 2). Adrenaline was not used with WT cells because there was already collected old data enough its effects to control cells. After baseline imaging, flecainide (10 µM) was flowed 3 minutes before recording (Figure 10A). No more than three cells were used from the same coverslip and it was washed 5 minutes with perfusate medium after flecainide before next baseline imaging of the same coverslip (Figure 10A and 10B).

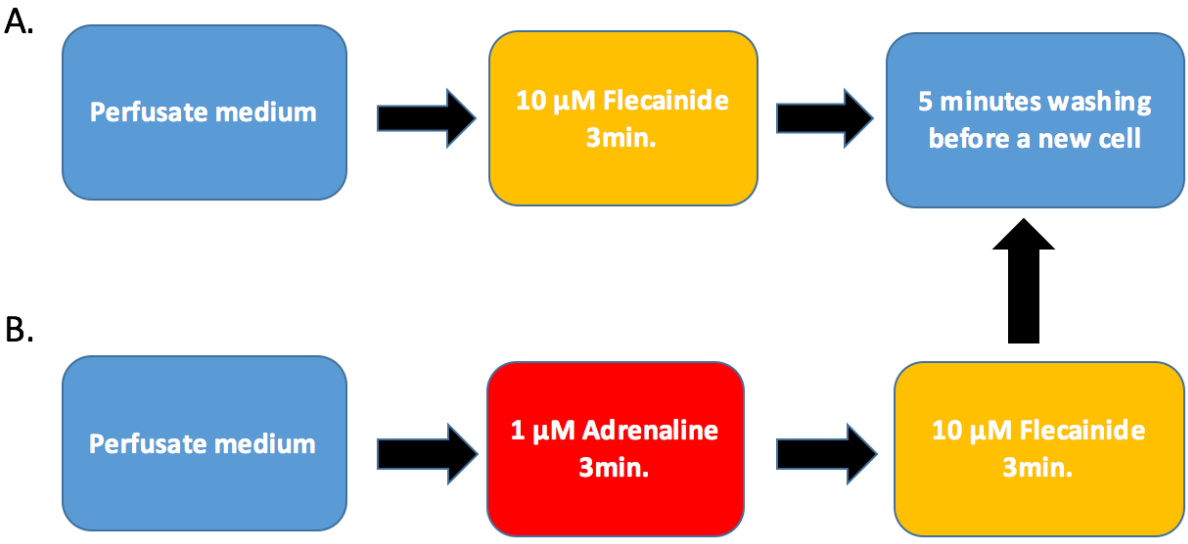


**Figure 11.** A) An imaging protocol of *UTA.04602.WT* cell line. B) An imaging protocol of *UTA.11705.SCN5A* and *UTA.13902.SCN5A* cell lines.

4.2.3.2 Drug experiments of *UTA.11705.SCN5A* and *UTA.13902.SCN5A* cell lines

In both experiments, beating areas were cut, dissociated and plated on coverslips. Dissociation was done 7 days before imaging in both imaging experiments. EB-culture medium (Table 2) was changed just once in week, one day before imaging. Cells of *UTA.13902.SCN5A* cell line were used 22 and 28 days after differentiation. Cells of *UTA.11705.SCN5A* were used 31 and 37 days after differentiation.

Experiments were started by recording baseline video with perfusate medium (Figure 11B). After baseline imaging, adrenaline with 1 µM concentration was used 3 minutes before imaging (Figure 11B). 10 µM of 5 mM adrenaline was dissolved to 50 ml of perfusate medium (Table 4) to get 1 µM concentration. After adrenaline imaging, 10 µM flecainide was flowed 3 minutes before recording (Figure 10B). Also with these cell lines, no more than three cells were used from the same coverslip and it was washed 5 minutes with perfusate medium after flecainide before next baseline imaging of a cell from the same coverslip (Figure 11A and 11B).

### 4.2.4 Beating analysis of cardiomyocytes

BeatView software is designed to analyze the contraction behaviour of single cardiomyocytes or their clusters (Ahola et al. 2014). It produces cell contraction and relaxation velocities as a function of time and calculates a number of cell contractile activity describing indicators. BeatView software has been developed as collaboration with Heart Group of University of Tampere and Computational Biophysics and Imaging Group of Tampere University of Technology. BeatView software versions 1.12 and 1.2 were used in this study.

From the recorded videos, the CMs were analyzed by manually cropping video at first and then selecting the cell of interest. After that, the region of interest (ROI) and the focus point of the beating movement were defined by eye. ROIs were divided into 8 sectors around the beating focus point. From each of these sectors, two sum vectors for velocity were calculated by the software (the radial and tangential component), resulting in 16 signals per cell (f12A). Beatview software creates 30 seconds raw signals of these sectors (Figure 12B). Three representative raw signals were selected for analysis.

The beating analysis were used to get different parameters from all of the videos: the time required for contraction, the time the cell remained contracted, the time needed for relaxation, possible incomplete relaxation phase and the time the cell remained relaxed (Figure 12C) as well as the beating frequency. BeatView software gives averages of parameters of these selected three sectors measurements. Version 1.2, which was launched during the project, also gives estimations of the regularity of the beating frequency and allows the user to flag abnormal or extra beats.

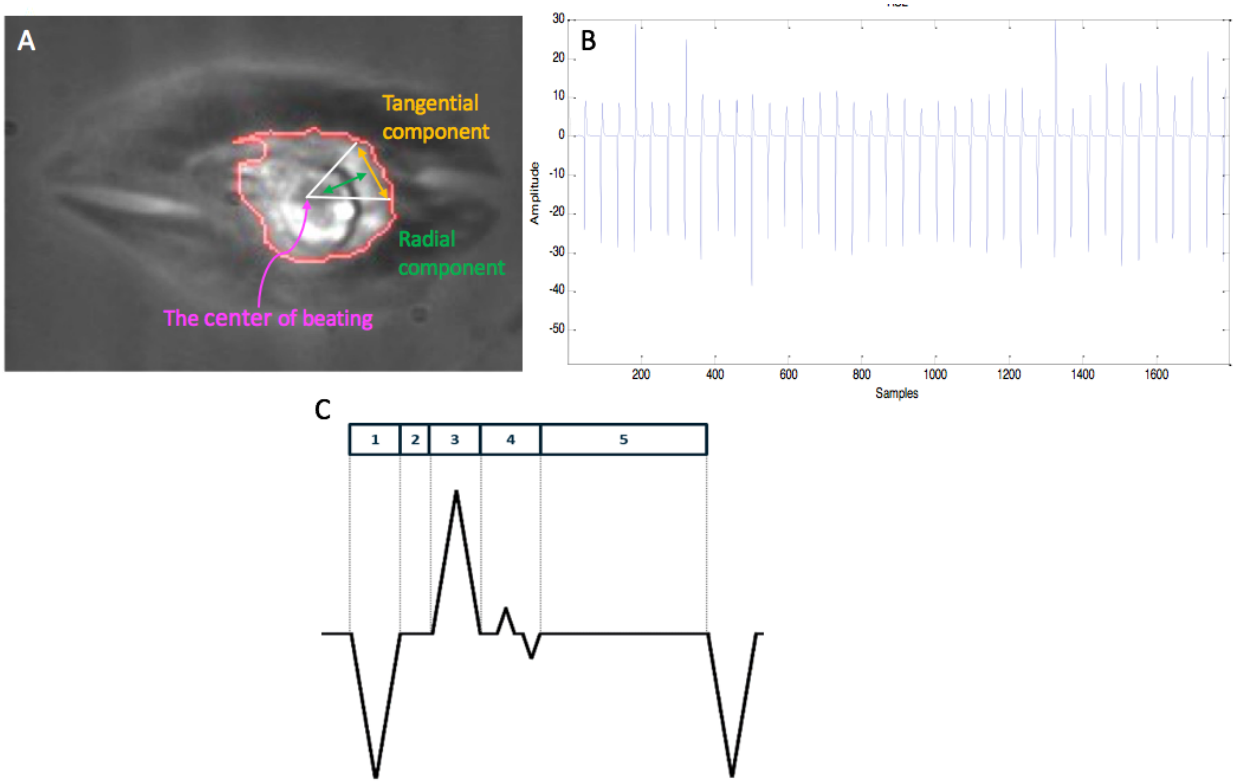


**Figure 12.** A) Selected cell with the analysis parameters shown. The center of beating movement (beating focus point) is marked with pink colour. Radial component is marked with green arrow and tangential component is marked with orange arrow. Red circle is the manually defined region of interest (ROI). B) 30 seconds signal of cell beating. C) Different phases of cardiac contraction/relaxation cycle: (1) the time of contraction, (2) the time the cell stayed contracted, (3) the time of relaxation, (4) incomplete relaxation and (5) the time the cell was relaxed.

### 4.2.5 Visual analysis of cardiomyocytes

Using the BeatView software proved to be impossible with some cases of the *SCN5A* cells because of their beating behaviour. Thus, also visual analysis of the beating was applied. In visual analysis, qualitative classification was used by visual inspection to all three cell lines. For this, 30 seconds videos were recorded of 33 of *UTA.11705.SCN5A*, 25 of *UTA.13902.SCN5A* and 26 of *UTA.04602.WT* cells. Based on the videos, cells were divided into six groups: 1) Regular, 2) Arrhythmic, 3) Vibrating, 4) Twisting, 5) Stopped beating, and 6) Other.

### 4.2.6 Statistical analysis

P values were calculated using non-parametric Mann-Whitney test with MS Excel.

# 5. Results

In this study, *SCN5A* mutation specific and WT hiPSC –derived CMs were imaged and analyzed both visually and using the BeatView software. *SCN5A* mutation –patient specific CMs were compared with WT CMs. Visual analyzing was used to get reliable data of those CMs, which were impossible to analyze with BeatView.

## 5.1 The analysis of the beating behaviour of single cardiomyocytes

### 5.1.1 Beating frequency

Beating behavior of single CMs was studied by using BeatView software. Beating of dissociated CMs was visualized with a microscope and their motion was video-recorded. Time required for each phase of beating was analyzed: the contraction, the time the cell stayed contracted, the relaxation time, and the time the cell stayed relaxed. The beating frequency was also measured and these results are presented in Figure 13. Figure 13A presents all cells' beating frequencies in normal conditions with perfusate medium. In both *SCN5A* cell lines the frequency was significantly higher ($p<0.05$) than in WT cells ($n=10$/each cell line). Figures 13B-D present all cell line beating frequencies with perfusate medium (baseline), adrenaline and flecainide. In all cell lines, flecainide significantly decreased ($p< 0.05$) beating frequency compared to baseline. Adrenaline slightly but significantly increased beating frequency of *UTA.11705.SCN5A* cells ($p<0.05$), but there was no statistically significant change with adrenaline in the beating frequency of *UTA.13902.SCN5A* cells ($p>0.05$).

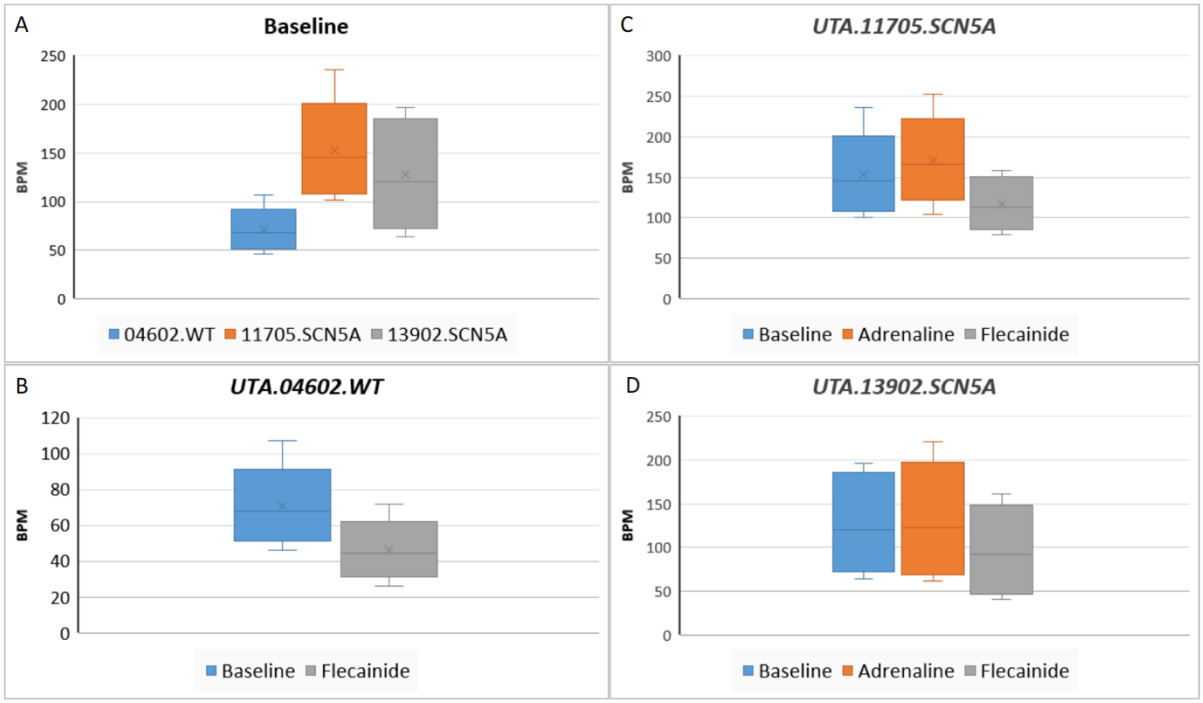


**Figure 13.** A) All cell lines' cells beating frequency with perfusate medium. B) *UTA.04602.WT* control cell lines cells beating frequency after perfusate medium (blue) and flecainide (grey). C) *UTA.11705.SCN5A* cell line beating frequency after perfusate medium (blue), adrenaline (orange) and flecainide (grey). D) *UTA.13902.SCN5A* cell line beating frequency after perfusate medium (blue), adrenaline (orange) and flecainide (grey). For all panels, beating frequencies are shown as beats per minute (BPM).

When comparing the *SCN5A* CMs to the WT CMs, average beating frequency was higher. Average beating frequency of WT cells were measured as 68 BPM and in *SCN5A* cells 146 BPM and 120 BPM with perfusate medium (Table 5). In *SCN5A* cells, adrenaline increased beating frequency 14.5 % and 1.2% on the average (Table 5). Flecainide decreased 34.6 % beating frequency in WT cells on the average, when in *SCN5A* cells, it decreased beating frequency 20.7 % and 23.5 %.

**Table 5.** Beating frequencies of all cell lines and the percentage changes.

| Cell line | Baseline (BPM) | Adrenaline (BPM) | Flecainide (BPM) | Change adrenaline/ baseline | Change flecainide/ adrenaline | Change flecainide/ baseline |
|---|---|---|---|---|---|---|
| *UTA.04602.WT* | 68 | - | 45 | - | - | -34.6 % |
| *UTA.11705.SCN5A* | 146 | 166 | 114 | 14.5 % | -30.8 % | -20.7 % |
| *UTA.13902.SCN5A* | 120 | 123 | 92.5 | 1.2 % | -24.2 % | -23.5 % |

5.1.2 Beat phase durations of cardiomyocytes

The durations of beat phases (mainly contraction and relaxation) were studied in all of cell lines (Table 6, Figure 14). For *UTA.04602.WT* CMs, adrenaline was not used after perfusate medium because it has studied earlier in Heart Group with different concentrations (0.1nM - 10uM) in WT cells. These earlier studies present that adrenaline increased 81 % beating frequencies on the average in WT cells with 1uM concentrations (personal communication). For WT cells, flecainide was added directly after perfusate medium. For *UTA.11705.SCN5A* and *UTA.13902.SCN5A* CMs, adrenaline was used after perfusate medium and flecainide was used after it. Figure 14 presents results of the video analysis received signals and average results of beat phase durations are shown in Table 6.

The sum displacement vectors were obtained from the video recordings, and several time parameters for different phases of beating were measured from these signals: (1) the time of contraction, (2) the time the cell stayed contracted, (3) the time of relaxation, (4) incomplete relaxation and (5) the time the cell was relaxed (Figure 14).

In WT CMs (n=10), average contraction and relaxation duration decreased after the addition of 10 μM flecainide versus perfusate medium (Table 6, Figure 14). Flecainide decreased contraction duration 5.2% and relaxation duration 4.7% on the average after baseline in WT CMs. Average time for the cell to be in a relaxed state increased 9.8% by flecainide and average time of total mechanical activity per beat increased 17.1% also by flecainide (Table 6, Figure 14).

Average contraction duration of *UTA. 11705.SCN5A* CMs (n=10) increased after 1 uM adrenaline 3% versus control medium and decreased 8.7% after 10 uM concentrations of flecainide (Table 6, Figure 14) versus adrenaline. Average relaxation duration with perfusate medium increased 4.7% after adrenaline and decreased 2.1% by flecainide (Table 6, Figure 14). Average time for the cell to be in a relaxed decreased 8.1% by adrenaline versus used perfusate medium and flecainide increased it 11% after adrenaline (Table 6, Figure 14). Adrenaline increased time of total mechanical activity per beat 1.7% after perfusate medium. After flecainide it increased 19.7% from 235 to 285 ms (Table 6, Figure 14).

Average contraction percentage of *UTA.13902.SCN5A* CMs (n=10) increased 2% after 1 uM adrenaline versus with perfusate medium and decreased 10.7% after 10 uM concentrations of flecainide (Table 6, Figure 14) after adrenaline. Average relaxation duration decreased 4.6% by adrenaline compared to with perfusate medium and decreased 3% by flecainide versus adrenaline (Table 6, Figure 14). Average time for the cell to be in a relaxed increased 3.3% by adrenaline versus used perfusate medium and flecainide also increased it 14% compared to adrenaline (Table 6, Figure 14). With perfusate medium time of total mechanical activity per beat decreased 3.2% from 341ms to 330ms after adrenaline and flecainide did not change it versus adrenaline (Table 6, Figure 14).

**Table 6.** Average durations of beat phases of all cell lines under different conditions.

| **Phase** | **Treatment** | ***UTA.04602.WT* (n=10)** | ***UTA.11705.SCN5A* (n=10)** | ***UTA.13902.SCN5A* (n=10)** |
|---|---|---|---|---|
| Contraction | Baseline | 163 ms (18.9 %) | 129 ms (31.0 %) | 149 ms (27.0 %) |
| | 1µM adrenaline | n.a. | 125 ms (34.0 %) | 158 ms (29.1 %) |
| | 10µM flecainide | 172 ms (13.7 %) | 134 ms (25.3 %) | 132 ms (18.3 %) |
| Relaxation | Baseline | 229 ms (26.9 %) | 106 ms (24.6 %) | 191 ms (33.9 %) |
| | 1µM adrenaline | n.a. | 112 ms (29.3 %) | 178 ms (29.3 %) |
| | 10µM flecainide | 286 ms (22.2 %) | 151 ms (27.2 %) | 197 ms (26.3 %) |
| Relaxed state | Baseline | 462 ms (54.2 %) | 201 ms (44.5 %) | 231 ms (38.1 %) |
| | 1µM adrenaline | n.a. | 144 ms (36.4 %) | 246 ms (41.4 %) |
| | 10µM flecainide | 867 ms (64.0 %) | 270 ms (47.4 %) | 475 ms (55.4 %) |
| Total mechanical activity per beat | Baseline | 392 ms | 235 ms | 341 ms |
| | 1µM adrenaline | n.a. | 239 ms | 330 ms |
| | 10µM flecainide | 459 ms | 286 ms | 330 ms |

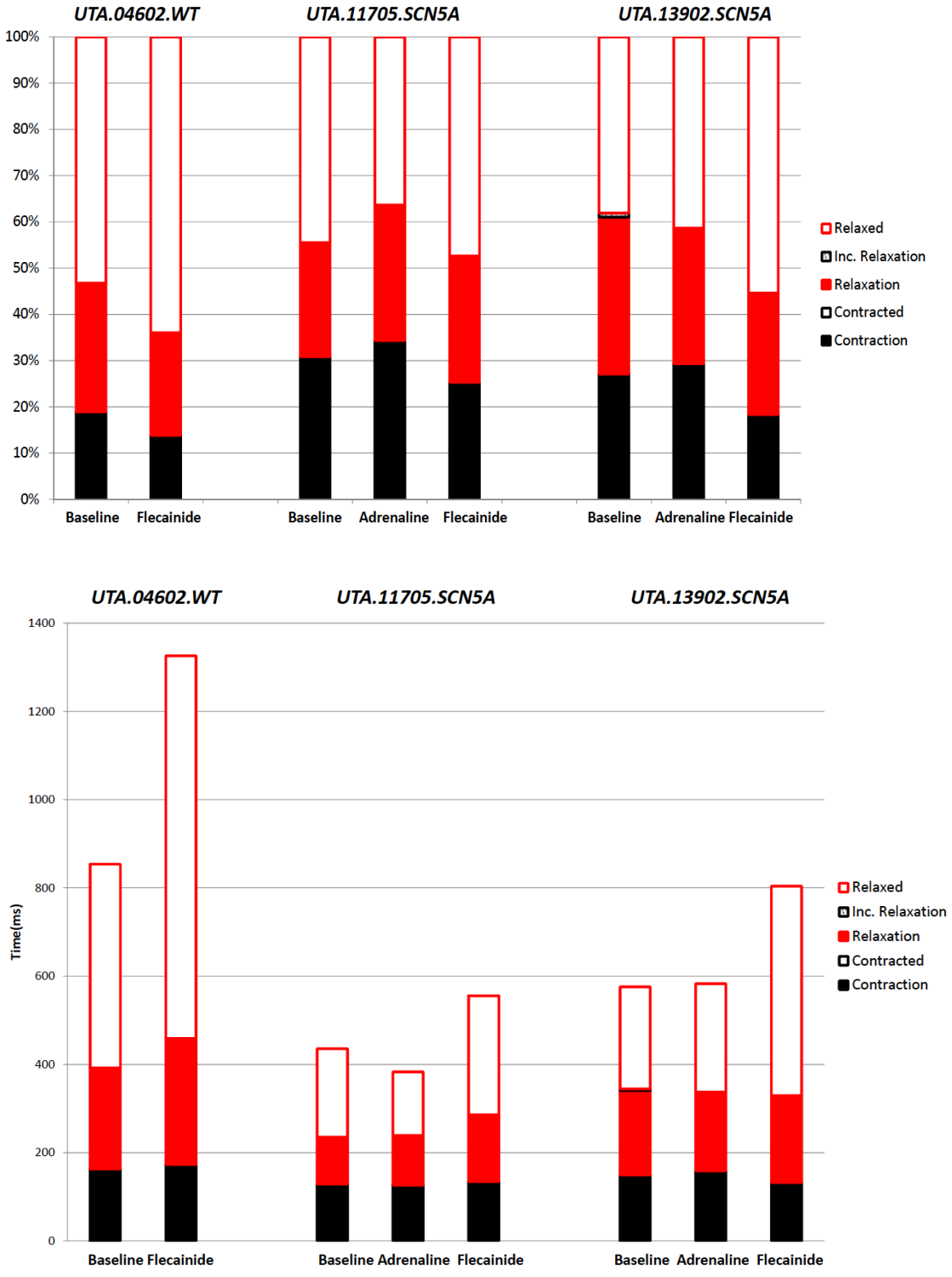


**Figure 14.** Illustrations of contraction-relaxation phases of all cell lines presented in Table 6. Upper graph presents phase durations as percentages of the one whole cardiac cycle and lower graph as milliseconds (ms). Different colors indicate different beat phases as shown next to the data columns.

## 5.2 Visual analyzing and classification of cardiomyocytes

Using the Beatview software proved to be impossible with some *SCN5A* cells because they could not be analyzed because of different reasons: 1) technical problems (irregular flow rate of perfusion), 2) cell's beating was too weak or the cell stopped beating (phenotypic for *SCN5A* cells), or 3) the beating movement was twisting and thus impossible to analyze using the software. Thus, these cells were analyzed by applying qualitative classification by visual inspection to all three cell lines. For this, 30 seconds videos were recorded of 33 of *UTA.11705.SCN5A*, 25 of *UTA.13902.SCN5A* and 26 of *UTA.04602.WT* cells. Based on the videos, cells were divided into six groups: 1) Regular, 2) Twisting, 3) Arrhythmic, 4) fibrillation, 5) Stopped beating, and 6) Other (Table 7). Figure 15 presents the results of the visual classification of all cell lines.

The group "Regular" included all regularly contracting cells regardless of beating frequency. The group "Twisting" consisted of cells whose beating was rather regular but the direction of the contraction and relaxation motion was not direct but rather circular or twisting. The group "Arrhythmic" contained cells whose beating was clearly irregular. The cells that did not have a clear resting phase but were beating quickly and continuously were classified as "Fibrillation". The group "Stopped beating" consisted of cells that stopped beating during the video recording because of stress caused by the recording conditions. The group "Other" contains cells that for example oscillated because of irregular flow rate of the perfusate, or did not fit in the other groups. Figure 15 presents percentages of CMs in the described categories for all cell lines.

**Table 7.** Classification of all cell lines after visual analyzing.

| | *UTA.11705.SCN5A* n=33 | *UTA.13902.SCN5A* n=25 | *UTA.04602.WT* n=26 |
|---|---|---|---|
| Regular | 6.1% | 8% | 23.1% |
| Twisting | 12.1% | 16% | 42.3% |
| Arrhythmic | 42.4% | 32% | 0% |
| Fibrillation | 15.2% | 12% | 0% |
| Stopped beating | 0% | 12% | 15.4% |
| Other | 24.2% | 20% | 19.2% |
| Total: | 100% | 100% | 100% |

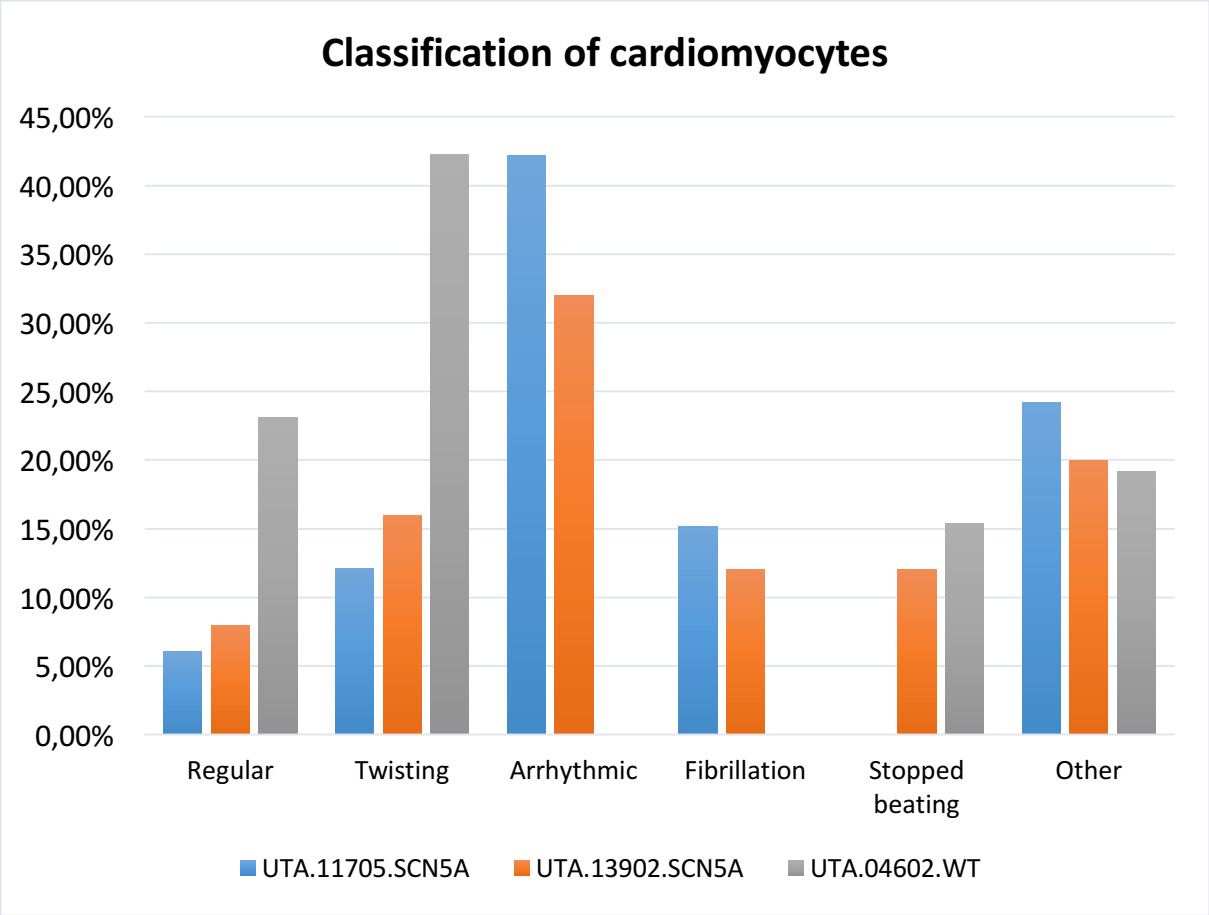


**Figure 15.** Classifications of cardiomyocytes of all cell lines. For some of the cells, classification was also possible with Beatview software. Cells were categorized by visual inspection and then data of Beatview software was reviewed. Visual inspection and Beatview software's data matched well. Figure 16 presents four different classes of CMs based both visual analyzing of the video and the data obtained from the Beatview software: a) Regular b) Twisting c) Arrhythmic and d) Fibrillation.

In Figure 16a), the regular beating rhythm and uniform beats are nicely visible. The signal can be also denser, but beating is regular. Figure 16b) the twisting movement is shown. The signal contains some doubled waves. When this type cell was visually inspected, it seems like cell beats upward with twisting movement. In Figure 16c) presents typical features of arrhythmic cell. The beats are uniform but the cell is stuck for a while and then continues beating again. Figure 16d) presents fibrillating beating where the signal seems like cell does not rest at all between two beats.

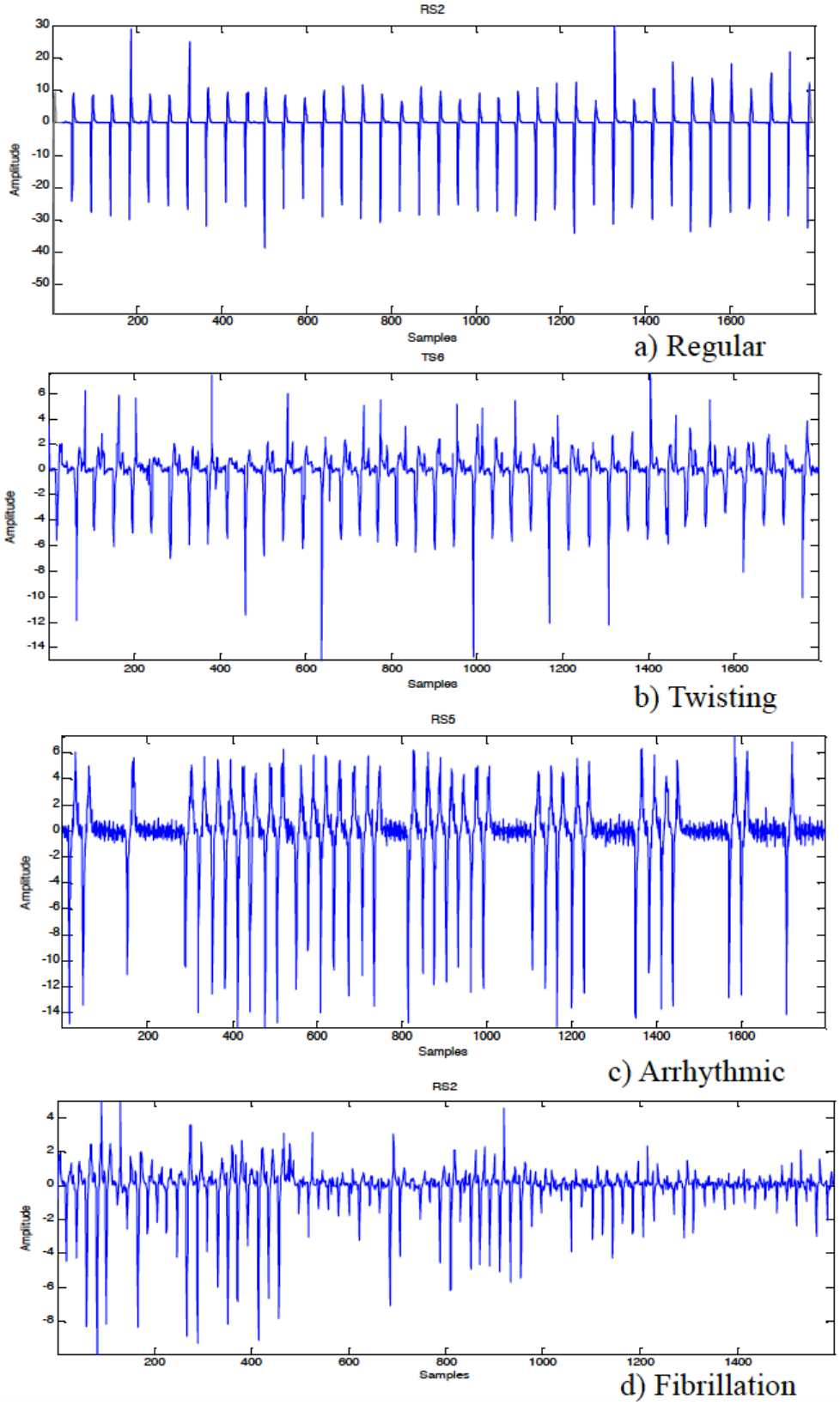


**Figure 16.** Different classifications based on data of Beatview software a) Regular cell's beating b) Twisting cell's beating c) Arrhythmic cell's beating d) Fibrillating cell's beating

# 6. Discussion

The aim of this study was to study iPS cell lines established from both control individual and patients carrying two different types of *SCN5A* mutations. The iPS cells were differentiated into cardiomyocytes and they were studied as *in vitro* models.

This study presents methods for analyzing CMs beating behavior both visually and with special developed software. Analysis is based on video recording of single beating CMs. Adrenaline is used to study *in vitro* arrhythmic symptoms of CMs with *SCN5A* mutations. Flecainide slow down the fast sodium channels in the atrial level, in chambers and in Purkinje fibers (Oulu & Tuomisto, 2007). It was used to study how it effects in good way to arrhythmic symptoms of the CMs.

In this study, one of the most important thing was to get well working set-up to analysis of the beating behavior of single cardiomyocytes. In Heart Group, cell line with *SCN5A* mutation p.141V *(UTA.11705.SCN5A)* has studied before with similar methods (Tuominen, 2015). In his study, the problem was that the effects of adrenaline. Adrenaline did not increase beating frequencies of CMs. This was most likely due to high baseline beating frequency of the cells. There were changes of pH temperature and moisture because well plate was moved back and forth between the microscope and the laminar. Medium was used to find out if it effects to beating frequencies of CMs.

## 6.1 Study setup

In this study, the drug effects on the cells were studied using perfusion. To build a reliable set-up, the first thing was to get a steady flow. It seemed that flow rate of perfusate effects to contrast of the video. If there were shaking or air bubbles during imaging, the Beatview software interpreted those as peaks. In those cases, manual editing of the analysis procedure was required. Control of the temperature was also very important.

## 6.2. Beating behaviours of single cardiomyocytes

In this study, CMs with *SCN5A* mutations were found to be beating more rapidly than WT cells. Perfusate medium was used to analyze the baseline beating behavior of the cells with

no drugs present. There are no earlier this kind of studies of *SCN5A* mutation cells' beating frequencies. It is known that patients with *SCN5A* mutations might have slower heart rate than usual and acceleration of the heart rate during exercise may be deficient (Toivonen et al. 2008). In this study, beating frequencies were almost two times higher in the *SCN5A* mutation carrying cells than in the WT cells. Adrenaline increases beating frequencies of individual CMs and especially I141V mutation cell line *(UTA.11705.SCN5A)* and this suitable for clinical picture of arrhythmias during exercise. Concentration (1μM) and duration of treatment were selected based on previous experience (personal communication in Heart Group).

Earlier studies in our group present that adrenaline works well with different concentrations (0.1nM-10 μM) in WT cells. These earlier studies present that adrenaline increased 81 % beating frequencies on the average in WT cells with 1uM concentrations (personal communication). For that, adrenaline was used to only CMs with *SCN5A* mutations. It did not increase so much beating frequencies as expected when analyzed with Beatview software. However, in visual analysis, adrenaline made disease cells more irregular. The adrenaline concentration was selected very high in order to see effects, but the higher doses did not change beating behaviors of the *SCN5A* cells.

Adrenaline is secreted during physical exertion. Patients with *SCN5A* mutations get arrhythmic symptoms during physical exercise when the heart rate is increased. This is why adrenaline was used to *SCN5A* cells in this study to see how it effects *in vitro*. Adrenaline effects by binding to adrenergic receptors. (Niensted et al. 2014.) Total adrenergic signaling in the heart is activated via both α- and β-adrenergic receptors, which results in stimulation of Protein kinase C (PKC) and Protein kinase A (PKA) signaling pathways, respectively (Chen et al. 2016). Earlier study presents that ADRA1A as the main α-adrenergic receptor isoform in adult ventricular cardiomyocytes, and human fetal fibroblasts, adult heart samples, as well as isolated adult ventricular myocytes showed abundant expression of ADRA1. They found that expression of ADAR1 mRNA was markedly downregulated during differentiation from all hESC and hiPSC lines. (Földes et al. 2014.)

In this earlier study it is also found that hiPSC-CM were in contrast unresponsive to phenylephrine, which is a selective $\alpha_1$-adrenergic receptor agonist.

Loss of phenylephrine response was independent from the cell line, cell culture conditions, reprogramming, and differentiating protocols they were used and was reproduced in different laboratories. Their study presented that cardiomyocytes differentiated from hESCs or hiPSCs did not measurably express the ADRA1A gene and ADRA1A mRNA was expressed (albeit modestly) in undifferentiated hESCs and hiPSCs but disappeared rapidly during differentiation to either cardiomyocytes or fibroblasts. (Földes et al. 2014.) Also β-Adrenergic signaling is considered to play a key role in regulating Ar$^{c}$hangels. A modern-day study characterized the properties of b-adrenergic signaling during in vitro differentiation and maturation of iPSC-CMs and confirmed active inotropic and chronotropic regulation in these models (Chen et al. 2016.). This could also be a reason for the lack of adrenergic effect in our cells.

These earlier studies support the idea that something might happen to adrenergic receptors after differentiation which might explain why adrenaline was not very effective in this study. This will inevitably affect the success and validity of studies. It would be crucial to find out what happens to adrenergic receptors during differentiation. Earlier studies also present that there are huge differences between mutual cell lines and also the age of the cells affected how they behave. (Zhu et al. 2014; Keung et al. 2014.)

Flecainide slows down the fast sodium channels in both the atrial level, that the chambers and in the Purkinje fibers (Koulu & Tuomisto, 2007). Our aim was to investigate whether flecainide would decrease the beating frequency and abolish arrhytmias of the *SCN5A* mutation carrying cells and this is exactly what was observed. Other studies have also presented that flecainide can effectively reduce exercise-induced ventricular arrhythmias in patients with CPVT, Andersen–Tawil syndrome (ATS) (Khoury et al. 2013; Delannoy et al. 2013, Watanabe et al.2009). Earlier study also presents that in carriers of *SCN5A* mutation, p.I141V carriers (in this study *UTA.11705.SCN5A)* who exhibited frequent multiformic premature ventricular complexes (PVCs) during exercise were subjected to exercise stress tests received help of flecainide. Flecainide significantly reduced the frequency of PVCs during and after exercise in this study. (Amarouch et al. 2016.) As well as previous studies that our study talks about beneficial effects of flecainide treatment also in *SCN5A* related arrhythmias.

There are not many published studies about R1913C mutation (in this study *UTA.13902.SCN5A* cell line). One patient with R1913C mutation was involved in study, which examined the relationship between repolarization abnormality and coved-type ST-segment elevation with terminal inverted T-wave (type 1 electrocardiogram [ECG]) in patients with Brugada syndrome (BrS) (Nagase et al. 2008). One of our patients *(UTA.13902.SCN5A)* was also a carrier of this R1913C mutation and presented Brugada type of clinical phenotype. According to our *in vitro* study, flecainide could reduce arrhythmias in this patient.

Our patients carried different mutations in the same *SCN5A* gene, but had completely different clinical symptoms. The experimental setup used in this this demonstrated increased amounts of arrhythmias in CMs derived from both of these individuals, but could not reveal any differences in them. More sophisticated analysis methods e.g. patch clamp are most likely needed to examine the precise electrical abnormalities caused by these two mutations.

In this study, flecainide decreased cells' beating frequency in all cell lines compared to adrenaline or control medium *in vitro*. Flecainide effects were noticed both by visually analyzing and by using Beatview software. Mutant cells can be analyzed much easier and faster than if patch clamp method is used. This study gives new data of both I141V and R1913C mutation. The clinical investigations of the affected patients, as well as the molecular and pharmacological characterization of the *SCN5A* mutation demonstrate that flecainide may serve as an effective treatment for the defect in Nav 1.5 that leads to an increased sodium window current (Amarouch et al. 2016). Flecainide is already in clinical use.

In addition to the presented drugs, the effect of antiepileptic drugs on the *SCN5A* cells would also be interesting to study. For example, rufinamide enhances the inactivation of sodium channels and shortens the QT interval (Wheless & Vazquez, 2010).

## 6.3 Beat phase durations of cardiomyocytes

In addition to beating frequency, durations of different beating phases of CMs were studied based on Beatview software data. Previous studies with LQT cells demonstrated that certain types of beating disorders can be detected at this level (Kiviaho et al. 2015) Our hypothesis

was that flecainide would increase the duration of the relaxation phase in all cell lines and adrenaline (was not used with WT cells) would increase the contraction time of *SCN5A* cells. In baseline, *SCN5A* cells had very short relaxation time compared to WT cells because of high beating frequencies. *UTA.11705.SCN5A* cells had significantly short relaxation time, but *UTA.13902* cells had similar relaxation time as in control CMs.

As already mentioned, adrenaline did not effect as assumed. It decreased the duration of the contraction phase in *UTA.11705.SCN5A* cell line but increased the relaxation phase duration. With *UTA.13902.SCN5A* cell line it increased a bit contraction phase duration and decreased relaxation phase duration. These unexpected effects might be due the above-mentioned study findings that adrenaline did not effects well with differentiated CMs because of adrenergic receptors.

Flecainide effected as assumed with all cell lines. In the WT cells its effect was the strongest. In the *UTA.13902.SCN5A* cell line it increased relaxation phase duration more than in *UTA.11705.SCN5A*. However, for both drugs (adrenaline and flecainide) have no clear change in beat phases were found. It can be said that these may affect the beating more on the general level than changing the duration of a specific phase. Certain types of cells (visually weak and slow beating) stopped beating during analysis, or beating weakened or otherwise becomes such that it could not be analyzed with Beatview. Weak beating, although not analyzable by the software, can be an important phenotype. Therefore, this result is a bit biased and it needs to repeat a larger cell population. In order to facilitate the analysis of the weak beating could use a higher magnification (40X, instead of now used 20X). Weak or stopped beating may be caused by the fact that the cells are relatively young. With more mature cells, the result may be different (Zhu et al. 2014; Keung et al. 2014).

## 6.4 Analyzing and classification of cardiomyocytes – arrhythmia analysis

Analyzing and classification of CMs were done both visually and using the Beatview software. The aim was to find out similarities and differences between analyzing visually or by using the Beatview software. Visual analyzing increased reliability of this study because with some *SCN5A* cells using the Beatview software proved to be impossible because of cell weakness or twisting, or problems in the set-up (see chapter 6.1 for details). Visual classification allows all beating subtypes to be analyzed.

Visual analyzing and classification were made of baseline videos using the perfusate medium. In visual analyzing, four matching classes with Beatview software were found: 1) Regular, 2) Regular, but twisting 3) Arrhythmic, 4) Fibrillation. Furthermore, two other groups were found by visually: 5) Stopped beating, and 6) Other. Similar groups were easy to notice by visually.

It was easy to distinguish differences between WT and *SCN5A* cells. Visually, WT cells were stronger and beat more regular compared to *SCN5A* cells. No arrhythmic beating behavior was detected. Notably, for the WT cells the category "Twisting" contained almost half of the cells. This might be due the strong beating or the immaturity of the cells. Twisting class was created due to software defects and this class may include also some normal cells. On the other hands, iPS-CMs are not mature because they are not elongated, but round and so their sarcomeric structure is not well organized (Bellin & Mummery, 2016). Cell shape affect strongly on how the beating movement looks like, and may cause the movement to appear twisting. Furthermore, there is a lot of discussion about cell's maturity affecting its behavior *in vitro*. One aspect would be assessing the possibility to use the twisting class as an indicator to determine how mature cells are.

In both *SCN5A* cell lines, the cells were smaller in size, they showed more arrhythmias or other abnormal beating behavior, and their overall beating appeared weaker than WT cells. SCN5A cells even had fibrillation. It is important to notice that the arrhythmic class was huge of *UTA.11705.SCN5A* CMs, from patient with I141V mutation. CMs with R1913C mutation *(UTA.13902.SCN5A)* behaviors more like WT than I141V mutation CMs. This finding describes clinical picture because as mentioned before, patients with this mutation had increasing amount of ventricular extra beats during exercise.

## 6.5 Beatview software

In this study, the Beatview software was used to study beating analysis with geometrical sectorial cell division and radial/tangential directions. The beating of dissociated stem cell-derived cardiomyocytes was visualized with a microscope and the motion was video-recorded (Ahola et al. 2014).

This study presents that it is easier to use software if video quality is sufficient. Incorrect lighting (too much or too little light) during video-recording makes video unusable. Furthermore, cell selection is a very important step. Selected cell should be strong enough, but too rigorous selection criteria can lead to miss important characteristic of phenotype like weak beating as this study presented.

As mentioned before, also perfusate flow rate influenced analyzing. If there were bubbles or shaking, it could be seen as an additional peak. Due to the update of the software, these extra spikes were easy to discard. The goal is to develop the software by following this studies challenges, such as the twisting cells, improve their analysis and thus get more exact results.

A major portion of the WT cells appeared regular but presented twisting in their beating behavior. This complicated the analysis using the Beatview software. The software assumes to have unidirectional contraction and relaxation phases, which is not true for twisting cells. For these cells, the signals showed double peaks which could not always be analyzed correctly. Software will be developed and the result of this study shows that this is an important point of development, and these findings also to help in this developing process. With *SCN5A* cells, the main problems were that they were beating so quickly and showed plenty of arrhythmias. Too dense beating rhythm complicated the analysis as the consecutive beats could not be separated from each other. If the software does not recognize all beats correctly, the signal cannot be analyzed reliably. For the arrhythmias, the 1.2 version of the software enabled better identification of arrhythmias and irregularities of cells. This property was developed specifically to meet the needs of this project.

## 6.6 Study limitations

In this method, it was important in set-up to get heating to be stable because cells react easily to even slight changes of temperature. If the temperature increased over 37’C or decreased under it, some CMs stopped beating. At high temperature quickly beating motion is often too weak to be analyzed without a recording setup of greater resolution power and lowering the temperature decreased CMs beating frequencies. (Laurila et al. 2016.) The present study also indicated that flowrate effects the temperature and so also beating. If liquid surface increased, temperature decreased and vice versa (Laurila et al. 2016). Controlling and awareness of

conditions are important things to get reliable results. In this study, was used to create reliable conditions for this type of analysis.

This study should continue to next level to Calcium imaging. Calcium ($Ca^{2+}$) is a universal intracellular second messenger. In muscle, $Ca^{2+}$ is best known for its role in contractile activation (Bers, 2008). $Ca^{2+}$ -imaging using fluorescent indicators is used to record beating frequency and diastolic calcium ion levels of cardiomyocytes during the baseline and adrenaline perfusion (Penttinen et al. 2015a).

## 6.7 Future challenges

It is well established that with single cell types, most often CMs, many cardiac diseases can be simulated. hiPSC- derived CMs are useful for modelling inherited human cardiac diseases since there are many different examples in which these cells phenocopy the pathogenic features of the disease. (Karakikes et, al. 2015.)

It is important to remember that the human heart is composed of vascular, smooth muscle and epicardial cells in addition to CMs. 3D cardiac tissue structures should be used to mime heart functions better and to typify interactions between different cell types may underlie the disease. (Bellin & Mummery, 2016.) Additionally, some diseases may benefit from developed culturing techniques, because some phenotypes might become evident only under optimized conditions (Birke et al. 2015). It has been also expected that complex multicellular structures will be necessary to present fully the pathology of the condition (Bellin & Mummery, 2016).

It is also estimated that in the future, iPSCs will find increasing usefulness when combined with cardiac tissue engineering (Bellin & Mummery, 2016). To mimic better multicellular and dynamic conditions of the cardiovascular system, one should also notice not only known or unknown genetic reasons but also issues related to ageing and drug-induced cardiac damage (Bellin & Mummery, 2016).

It is expected that to model different dynamics that effect blood flow, mechanical stretch and the electrical stimulations leads to structurally and functionally mature human myocardium (Bellin & Mummery, 2016). Biological and biophysical readouts that allow high throughput,

real-time and quantitative measurement of cardiac (patho)physiological status can be built to this myocardium. This can enable studying how the human heart reacts to toxic compounds and disease, enhance the integrity of the disease models, and refine the predictability of drug responses (Bellin & Mummery, 2016).

At the same time, a big promise is a big challenge: disease treatment and prevention can be tailored to the individual with hiPSC technology because hiPSCs represent the genetic background of the person. The goal is to utilize hiPSC- derived CMs in personalized medicine based on their accomplishments to predict patients' response to administered drugs. In the next few years, hiPSC-CMs based studies should be able to find out applying the same drug to patients' hiPSC-CMs, and following-up over time the patients whether the *in vitro* responses matched the final clinical outcome (Bellin & Mummery, 2016). Previous studies in our group presents this with genetic ventricular tachycardia (Catecholaminergic polymorphic ventricular tachycardia, CPVT) –derived CMs (Penttinen et al. 2015).

It would be an ideal combination if all of parameters including the structural, molecular and electrophysiological characteristics associated with CM maturation could be estimated to determine how well the hiPSC-derived CMs resemble myocytes of the human adult heart (Bellin & Mummery, 2016). It has been estimated that late hiPSC-CMs (>35 days) are at the maturity level of the cardiomyocytes of embryos, but they have similar to the dimensions of human embryonic CM but remain small compared to adult (Robertson et al. 2013). It is usual to test only some of these parameters, especially those that are most important for the disease phenotype to be estimated (Bellin & Mummery, 2016).

It would be also important to find out the physiological processes of maturation and ageing that the heart naturally experiences from its formation to birth and during the lifespan of a human being *in vitro* conditions (Veerman et al. 2015; Van meer and Mummery, 2016). Because the heart contracts many millions time over a lifetime, aging reveals defects in CMs. Maturation is not understood fully. It clearly requires environmental factors like hormones, exercise and CM growth by hypertrophy. Prolonged culture, metabolic manipulation, tissue engineering technologies, electromechanical pacing and other biophysical approaches are used to utilize these issues. (Veerman et al. 2015; Van meer and Mummery, 2016.)

An important question is how do we recognize in mature CM in a culture dish. The structural, molecular and electrophysiological characteristic are ideally combination of parameters associated with CM maturation. These parameters should be assessed to determine whether hiPSC-CMs resemble myocytes of the human adult heart (Bellin & Mummery, 2016; Robertson et al. 2013). It is typical to practice to test only some of these parameters, usually only those that are most important for the disease phenotype to be assessed.

All aspects of functionality of the cells, including electrophysiology, calcium handling properties, patterns and force of contraction, should be measured (Bellin & Mummery, 2016). It is possible, that in future there will be application of hiPSC-CMs which would estimate their maturation and also 2D and 3D settings will become a useful tool for disease modelling and drug testing, as well as for testing conditions that may eventually enhance maturation. Other variables, which have an effect to the CM growth, such as substrate stiffness and specific molecular cues, need to be determined. It is still indistinct whether an adult phenotype will ever be completely achieved *in vitro* (Bellin & Mummery, 2016).

# 7. Conclusions

In this study, baseline beating characterization and drug responses of hiPSC –derived cardiomyocytes (CMs) carrying mutation *SCN5A* were studied with different methods. They were compared to wild type (WT) cells from a healthy individual. *SCN5A* mutation –patient specific and WT iPSC –derived CMs were imaged and analysed both visually and using the BeatView software.

At baseline the beating behaviors of diseased cells were more arrhythmic than that of control cells and beating frequencies was higher than in control cells. This describes well clinical picture of how patients suffering from arrhythmias. The time the cells were relaxed was also shorter time than in control cells. Flecainide slowed down the beating frequency and increased the time cells were relaxed in all cell lines, as expected but adrenaline did not increase bf as well we assumed. Visual analysing was needed to use to get more reliable data of the CMs, which are impossible to analyze with the BeatView software.

More studies of the functionality, morphology and maturity of hiPSC –derived CMs are needed in the future to find out the true potential of hiPSC –applications in cardiac disease modeling. Because hiPSCs represent the genetic background of the person, disease treatment and prevention can be tailored to the individual with hiPSC technology. Better differentiation methods, tissue engineering studies, advanced culturing conditions and more developed software is needed to get more mature hiPSC-CMs for cardiac regenerative medicine.

# 8. References


Amarouch MY, Swan H, Leinonen J, Marjamaa A, Lahtinen AM, Kontula K, Toivonen L, Widen E and Abriel H: Antiarrhythmic Action of Flecainide in Polymorphic Ventricular Arrhythmias Caused by a Gain-of-Function Mutation in the Nav 1.5 Sodium Channel. Ann Noninvasive Electrocardiol. 2016 Jul;21(4):343-51. doi: 10.1111/anec.12312.

Amarouch M.-Y., Kasimova M. A., Tarek M., Abriel H. (2014). Functional interaction between S1 and S4 segments in voltage-gated sodium channels revealed by human channelopathies. Channels. 2014; 8(5) 414–420.

Barefield D, Kumar M, de Tombe PP, Sadayappan S. Contractile dysfunction in a mouse model expressing a heterozygous MYBPC3 mutation associated with hypertrophic cardiomyopathy. Am J Physiol Heart Circ Physiol. 2014;306(6):807-15.

Bellin M and Mummery CL: Inherited heart disease - what can we expect from the second decade of human iPS cell research? FEBS Lett. 2016;590(15):2482-93. doi: 10.1002/1873-3468.12285.

Bellin M, Marchetto MC, Gage FH, Mummery CL. Induced pluripotent stem cells: the new patient? Nature Reviews Molecular Cell Biology 2012;13:713-726.

Bennett PB, Yazawa K, Makita N, George AL. Molecular mechanism for an inherited cardiac arrhythmia. Nature. 1995;376:683–685.

Bers DM. Calcium Cycling and Signaling in Cardiac Myocytes. Annu. Rev. Physiol. 2008. 70:23–49.

Bers DM. Calcium Fluxes Involved in Control of Cardiac Myocyte Contraction. Circ Res. 2000;87:275-281.

Bers DM. Excitation-contraction coupling and cardiac contractile force. 2nd edition, Kluwer academic
publishers, Dordrecht, 2001.

Birket MJ, Ribeiro MC, Kosmidis G, Ward D, Leitoguinho AR, van de Pol V, Dambrot C, Devalla HD, Davis RP, Mastroberardino PG, Atsma DE, Passier R and Mummery CL:Contractile defect caused by mutation in MYBPC3 revealed under conditions optimized for human PSCcardiomyocyte function. Cell Rep. 2015;13(4):733-45. doi: 10.1016/j.celrep.2015.09.025.

Bjålie JG, Haug E, Sand O, Sjaastad OV. Ihmisen fysiologia ja anatomia.1-5 painos. WSOY 2008.

Boron W.F, Boulpaep E.L, Medical physiology: A Cellular and Molecular Approach, 2nd edition. Saunders Elsevier, 2009.

Bootman MD, Higazi DR, Coombes S, Roderick HL. Calcium signalling during excitation-contraction coupling in mammalian atrial myocytes. J Cell Sci. 2006;119(19):3915-25.

Brugada P, Brugada J. Right bundle branch block, persistent ST segment elevation and sudden cardiac death: A distinct clinical and electrocardiographic syndrome. J Am Coll Cardiol 1992, 20: 1391-1396.
Brugada R, Campuzano O, Sarquella-Brugada G, Brugada J, Brugada P: BRUGADA SYNDROME. Methodist Bebakey Cardiovasc J. 2014;10(1):25-28.

Butters, T.D., Oleg V. Aslanidi, Inada S, Boyett M.R, Hancox JC, Lei M and Zhang H: Mechanistic links between Na+ channel (*SCN5A*) mutations and impaired cardiac pacemaking in sick sinus syndrome. Circ. Res. 2010;107 (1), 126–137.

Chen IY, Matsa E and Wu JC: Induced pluripotent stem cells: at the heart of cardiovascular precision medicine. Nat Rev Cardiol. 2016 Jun;13(6):333-49. doi: 10.1038/nrcardio.2016.36.

Chen-Izu Y, Shaw RM, Pitt GS, Yarov-Yarovoy V, Sack JT, Abriel H, Aldrich RW, Belardinelli L, Cannell MB, Catterall WA, Chazin WJ, Chiamvimonvat N, Deschenes I, Grandi E, Hund TJ, Izu LT, Maier LS, Maltsev VA, Marionneau C, Mohler PJ, Rajamani S, Rasmusson RL, Sobie EA, Clancy CE, Bers DM: Na+ channel function, regulation, structure, trafficking and sequestration. The Journal of Physiology. 2015;593 (6): 1347–60.

Chen Q, Kirsch GE, Zhang D, Brugada R, Brugada J, Brugada P, Potenza D, Moya A, Borggrefe M, Breithardt G, Ortiz-Lopez R, Wang Z, Antzelevitch C, O'Brien RE, Schulze-Bahr E, Keating MT, Towbin JA, Wang Q. Genetic basis and molecular mechanism for idiopathic ventricular fibrillation. Nature. 1998;392:293–296.

Chiu C, Bagnall RD, Ingles J, Yeates L, Kennerson M. Mutations in alpha-actinin-2 cause hypertrophic cardiomyopathy: a genome-wide analysis. J Am Coll Cardiol. 2010;55(11):1127-35.

Clark KA, McElhinny AS, Beckerle MC, Gregorio CC. Striated muscle cytoarchitecture: an intricate web of form and function. Annu Rev Cell Dev Biol. 2002;18:637-706.

Dehaan RL, Eichna LW. Differentiation of the atrioventricular conducting system of the heart. Circulation. 1961;24:458-70.

Delannoy E, Sacher F, Maury P, Mabo P, Mansourati J, Magnin I, Camous JP, Tournant G, Rendu E, Kyndt F, Haïssaguerre M, Bézieau S, Guyomarch B, Le Marec H, Fressart V, Denjoy I, Probst V: Cardiac characteristics and long-term outcome in Andersen-Tawil syndrome patients related to KCNJ2 mutation. Europace. 2013 Dec;15(12):1805-11. doi: 10.1093/europace/eut160.

Escárcega RO, Jiménez-Hernández M, Garcia-Carrasco M, Perez-Alva JC, Brugada J. The Brugada syndrome. Acta Cardiol. 2009;64:795–801.

Földes G, Matsa E, Kriston-Vizi J, Leja T, Amisten S, Kolker L, Kodagoda T, Dolatshad NF, Mioulane M, Vauchez K, Arányi T, Ketteler R, Schneider MD, Denning C and Harding SE: Aberrant α-adrenergic hypertrophic response in cardiomyocytes from human induced pluripotent cells. Stem Cell Reports. 2014 Nov 11;3(5):905-14. doi: 10.1016/j.stemcr.2014.09.002.

Harris SP, Lyons RG, Bezold KL. In the Thick of It: HCM-Causing Mutations in Myosin Binding Proteins of the Thick Filament. Circ Res. 2011;108:751-764.

Hedley PL, Jørgensen P, Schlamowitz S, Wangari R, Moolman-Smook J, Brink PA, Kanters JK, Corfield VA, Christiansen M. The genetic basis of long QT and short QT syndromes: a mutation update. Hum Mutat. 2009;30(11):1486-511.

Heikkilä J, Kupari M, Airaksinen H, Huikuri, M. Nieminen S, and Peuhkurinen K. Kardiologia, 2 painos. Kustannus Oy Duodecim 2008.

Jiang C, Atkinson D, Towbin JA, Splawski I, Lehmann MH, Li H, Timothy K, Taggart RT, Schwartz PJ, Vincent GM. Two long QT syndrome loci map to chromosomes 3 and 7 with evidence for further heterogeneity. Nat Genet. 1994;(8):141–147.

Karakikes I, Ameen M, Termglinchan V, and Wu JC: Human Induced Pluripotent Stem Cell-Derived Cardiomyocytes: Insights into Molecular, Cellular, and Functional Phenotypes. Circ Res. 2015; 117(1): 80–88. doi: 10.1161/CIRCRESAHA.117.305365

Keung W, Boheler KR, Li RA. Developmental cues for the maturation of metabolic, electrophysiological and calcium handling properties of human pluripotent stem cell derived cardiomyocytes. Stem Cell Res Ther. 2014;5(1):17.

Khoury A, Marai I, Suleiman M, Blich M, Lorber A, Gepstein L, Boulos M: Flecainide therapy suppresses exercise-induced ventricular arrhythmias in patients with CASQ2-associated catecholaminergic polymorphic ventricular tachycardia. Heart Rhythm. 2013 Nov;10(11):1671-5. doi:10.1016/j.hrthm.2013.08.011.

Kiviaho, A, Ahola A, Larsson K, Penttinen K, Swan H, Pekkanen-Mattila M, Venäläinen H, Paavola K, Jari Hyttinen J and Aalto-Setälä, K: Distinct electrophysiological and mechanical beating phenotypes of long QT syndrome type 1-specific cardiomyocytes carrying different mutations. IJC Heart & Vasculature. 2015;8; 19–31.

Koulu M and Tuomisto J. Farmakologia ja toksikologia. 7 Uudistettu painos. Kustannusosakeyhtiö MEDICINA Kuopio 2007.

Kujala K, Paavola J, Lahti A, Larsson K, Pekkanen-Mattila M, et al. Cell Model of Catecholaminergic Polymorphic Ventricular Tachycardia Reveals Early and Delayed Afterdepolarizations. PLoS ONE 2012;7(9):e44660.

Kusuda-Furue M, Tateyama D, Kinehara M, Na J, Okamoto T, Sato JD: Advantages and difficulties in culturing human pluripotent stem cells in growth factor-defined serum-free medium. In Vitro Cell Dev Biol Anim. 2010;46(7):573-6.

Lan F, Lee AS, Liang P et al. Abnormal Calcium Handling Properties Underlie Familial Hypertrophic Cardiomyopathy Pathology in Patient-Specific Induced Pluripotent Stem Cells. Cell Stem Cell 2013;12:101–113.

Laurila E, Ahola A, Hyttinen J and Aalto-Setälä K: Methods for in vitro functional analysis of iPSC derived cardiomyocytes - Special focus on analyzing the mechanical beating behavior. Biochim Biophys Acta. 2016;1863(7 Pt B):1864-72.

Lian X, Zhang J, Azarin SM, Hazeltine LB, Bao X, Hsiao C, Kamp TJ, Palecek SP: Directed cardiomyocyte differentiation from human pluripotent stem cells by modulating Wnt/β-catenin signaling under fully defined conditions. 2013; Nature Protocols (8):162–175.

Liu M, Yang KC, and Dudley S.D, Jr: Cardiac sodium channel mutations: why so many phenotypes? Nat Rev Cardiol. 2014; 11(10): 607–615.

Malan D, Friedrichs S, Fleischmann BK, and Sasse P.:Cardiomyocytes obtained from induced pluripotent stem cells with long-QT syndrome 3 recapitulate typical disease-specific features in vitro. Circ Res. 2011;109(8):841-7.

Moorman AF, Christoffels VM. Cardiac chamber formation: development, genes, and evolution. Physiol Rev. 2003;83(4):1223-67.

Mummery C, Ward-van Oostwaard D, Doevendans P, Spijker R, van den BS, Hassink R, et al. Differentiation of human embryonic stem cells to cardiomyocytes: role of coculture with visceral endoderm-like cells. Circulation. 2003;107:2733–2740.

Mummery CL, Zhang J, Ng ES, Elliott DA, Elefanty AG, Kamp TJ. Differentiation of Human Embryonic Stem Cells and Induced Pluripotent Stem Cells to Cardiomyocytes: A Methods Overview. Circ Res. 2012;111:344-358.

Nagase S, Kusano KF, Morita H, Nishii N, Banba K, Watanabe A, Hiramatsu S, Nakamura K, Sakuragi S and Ohe T: Longer repolarization in the epicardium at the right ventricular outflow tract causes type 1 electrocardiogram in patients with Brugada syndrome. J Am Coll Cardiol. 2008;51(12):1154-61. doi: 10.1016/j.jacc.2007.10.059.

Niensted W, Hänninen O, Arstila A, Björkqvist S-E : Ihmisen fysiologia ja anatomia. 19 uudistettu painos. Sanoma Pro, 2014.

Obeyesekere MN, Antzelevitch C and Krahn AD: Management of Ventricular Arrhythmias in Suspected Channelopathies. Circulation: Arrhythmia and Electrophysiology. 2015;8:221-231

Ojala M, Rajala K, Pekkanen-Mattila M, Miettinen M, Huhtala H and Aalto-Setälä K: Culture Conditions Affect Cardiac Differentiation Potential of Human Pluripotent Stem Cells: PLoS One. 2012; 7(10).

Penttinen K, Swan H, Vanninen S, Paavola J, Lahtinen A.M, Kontula K, Aalto-Setälä K: Antiarrhythmic Effects of Dantrolene in Patients with Catecholaminergic Polymorphic Ventricular Tachycardia and Replication of the Responses Using iPSC Models: PLoS One. 2015; 10(5): e0125366.

a) Penttinen K, Siirtola H, Àvalos-Salguero J, Vainio T, Juhola M, and Aalto-Setälä K;
Novel Analysis Software for Detecting and Classifying Ca2+ Transient Abnormalities in Stem Cell-Derived Cardiomyocytes. PLoS One. 2015;26;10(8):e0135806.

Remme C. Cardiac sodium channelopathy associated with *SCN5A* mutations: electrophysiological, molecular and genetic aspects: J Physiol. 2013 Sep 1;591(17):4099-116, 2013.

Robertson C, Tran DD, George SC. Concise review: maturation phases of human pluripotent stem cell-derived cardiomyocytes. Stem Cells. 2013;31(5):829-37.

Sadahiro T., Yamanaka S., Ieda M. Direct cardiac reprogramming: progress and challenges in basic biology and clinical applications. Circ. Res. 2015;116:1378–1391.

Severs NJ. The cardiac muscle cell. Bioessays. 2000;22(2):188-99.

Splawski I, Shen J, Timothy KW, Lehmann MH, Priori S, Robinson JL, Moss AJ, Schwartz PJ, Towbin JA, Vincent GM and Keating MT: Circulation. 2000;102(10):1178-85.

Srivastava D and Yu P: Recent advances in direct cardiac reprogramming. Curr Opin Genet Dev. 2015;34:77-81.

Sun N, Yazawa M, Liu J, Han L, Sanchez-Freire V, Abilez OJ et al. Patient-specific induced pluripotent stem cells as a model for familial dilated cardiomyopathy. Sci Transl Med. 2012;4(130):130-47.

Swan H, Amarouch Y, Leinonen J, Marjamaa A, Kucera J.P, Laitinen-Forsblom P.J, Lahtinen A.M, Palotie A, Kontula K, Toivonen L, Abriel and Widen W: Gain-of-Function Mutation of the *SCN5A* Gene Causes Exercise-Induced Polymorphic Ventricular Arrhythmias, Circ Cardiovasc Genet. 2014;7:771-781.
Swan H, Piippo K, Viitasalo M et al (1999) Arrhythmic disorder mapped to chromosome 1q42-q43 causes malignant polymorphic ventricular tachycardia in structurally normal hearts. J Am Coll Cardiol 1999;34:2035–2042

Takahashi K, Tanabe K, Ohnuki M, Narita M, Ichisaka T et al. Induction of pluripotent stem cells from adult human fibroblasts by defined factors. Cell. 2007;131(5):861-72.

Takahashi K, Yamanaka S. Induction of pluripotent stem cells from mouse embryonic and adult fibroblast cultures by defined factors. Cell. 2006;126(4):663-76.

Tardiff JC. Thin Filament Mutations Developing an Integrative Approach to a Complex Disorder. Circ Res. 2011;108:765-782.
Thaler MS: The Only EKG Book You'll Ever Need. Philadelphia: Lippincott Williams & Wilkins, 1999.

Toivonen L, Swan H, Viitasalo M, ym. Pitkä QT-oireyhtymä: kansallinen suositus. Duodecim 2008;124(8):902-12.

Van Meer BJ, Tertoolen LG and Mummery CL: Concise Review: Measuring Physiological Responses of Human Pluripotent Stem Cell DerivedCardiomyocytes to Drugs and Disease. Stem Cells. 2016 ;34(8):2008-15. doi: 10.1002/stem.2403.

Veerman CC, Kosmidis G, Mummery CL, Casini S, Verkerk AO and Bellin M: Immaturity of human stem-cell-derived cardiomyocytes in culture: fatal flaw or soluble problem? Stem Cells Dev. 2015 May 1;24(9):1035-52. doi: 10.1089/scd.2014.0533.

Vijayakumar R, Silva JN.A, Desouza KA, Abraham RL, Strom M, Sacher F, Van Hare GF, Haïssaguerre M,. Roden DM and Yoram Rudy: Electrophysiologic Substrate in Congenital Long QT Syndrome Noninvasive Mapping With Electrocardiographic Imaging (ECGI). Circulation. 2014;130:1936-1943.

Veltmann C, Barajas-Martinez H, Wolpert C, Borggrefe M, Schimpf R, Pfeiffer R, Cáceres G, Burashnikov E, Antzelevitch C, Hu D: Further Insights in the Most Common *SCN5A* Mutation Causing Overlapping Phenotype of Long QTSyndrome, Brugada Syndrome, and Conduction Defect. J Am Heart Assoc. 2016; 5;5(7).

Watanabe H, Chopra N, Laver D, Hwang HS, Davies SS, Roach DE, Duff HJ, Roden DM, Wilde AA and Knollmann BC: Flecainide prevents catecholaminergic polymorphic ventricular tachycardia in mice and humans. Nat Med. 2009;15(4):380-3. doi: 10.1038/nm.1942.

Wheless JW, and Vazquez B,: Rufinamide: A Novel Broad-Spectrum Antiepileptic Drug. Epilepsy Curr. 2010; 10(1): 1–6. doi: 10.1111/j.1535-7511.2009.01336.x

Wilde AA and Brugada R. Phenotypical manifestations of mutations in the genes encoding subunits of the cardiac sodium channel. Circ Res. 2011;108:884–897.

Zhu R, Blazeski A, Poon E, Costa KD, Tung L and Boheler KR: Physical developmental cues for the maturation of human pluripotent stem cell-derived cardiomyocytes. Stem Cell Res Ther. 2014 Oct 20;5(5):117. doi: 10.1186/scrt507.